10064 - Physics Project

The dielectrophoretic force on dielectric spherical objects

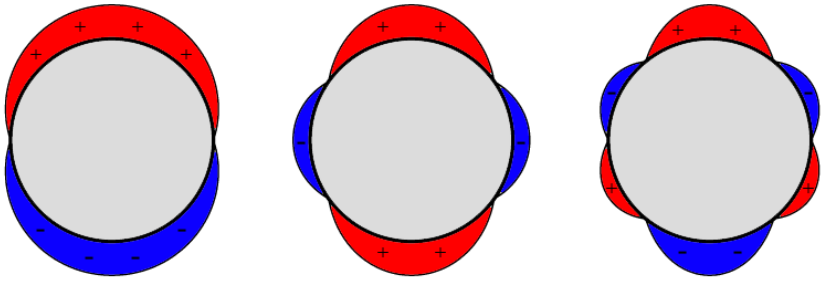

Andreas Ammitzbøll s042191

Janosch Michael Cristoph Rauba s042606

Marco Haller Schultz s042357

Supervisors: Niels Asger Mortensen and Henrik Bruus

MIC – Department of Micro and Nanotechnology
Technical University of Denmark

21 June 2006

Abstract

We have studied the dielectrophoretic force on dielectric spherical objects immersed in a dielectric medium and subject to a non uniform externally applied electric field. We derived an exact expression for the dielectrophoretic force in the case where the external field was azimuthal symmetric and expressed as an infinite sum of Legendre Polynomials. The expression for the force was then also given as an infinite sum and the n'th term turned out to represent the force on the induced multipole of order $n+1$. The lowest term in the sum represented the lowest order approximation of the dielectrophoretic force.

A comparison of the lowest-order approximation and the exact result was made. Here we explicitly studied the error involved in using the approximation in cases where the external field was that of a dipole or that of a point charge. The lowest order approximation turned out to dominate in cases where the electric field was approximatively uniform over the diameter of the object considered. We saw that in cases where the object was placed in a very non uniform electric field, higher order terms dominated.

We then developed the theory for a simple cell model, a dielectric sphere consisting of two layers of dielectric media with different permittivities. We saw that it was possible to define an effective permittivity which reduced the problem of considering a sphere consisting of two layers to a problem where we only had to consider one layer. A comparison of the force on two such spheres was conducted. We found that for large distances between field source and object the force differed only by a multiplicative constant.

The behavior of the spherical objects in an AC potential was considered. It turned out that the critical frequencies, i.e. the frequency were the dielectrophoretic force is zero, is different for all induced multipole moments. In the case of an inhomogeneous electric field one therefore had to describe a spherical object with an interval of critical frequencies.

A simple and artificial simulation of the trajectory of an dielectric spherical object in a microchannel was then done by solving the equation of motion of the object. The simulation illustrated the frequency dependence of positive and negative dielectrophoresis.

Contents

List of Figures

List of Tables

List of symbols

Symbol	Description	Unit
Δp	Pressure drop	$\mathrm{kg/ms^2}$
$\mathrm{d}\tau$	Infinitesimal volume element	$\mathrm{m^3}$
$\mathrm{d}a$	Infinitesimal element of area	$\mathrm{m^2}$
σ_{el}	Electric conductivity	S/m
ω	Angular frequency	rad/s
ρ	Mass density	$\mathrm{kg\ m^{-3}}$
ρ_t	Volume charge density, total	$\mathrm{C/m^3}$
ρ_f	Volume charge density, free	$\mathrm{C/m^3}$
ρ_b	Volume charge density, bound	$\mathrm{C/m^3}$
σ	Surface charge density, bound	$\mathrm{C/m^2}$
ϵ_0	Permittivity of the free space	$\mathrm{C^2/Nm^2}$
ϵ	Permittivity	$\mathrm{C^2/Nm^2}$
ϵ_r	Relative permittivity	-
χ_e	Electric susceptibility	-
$\mathbf{P}$	Dipole moment per volume	$\mathrm{C/m^2}$
p	Magnitude of the dipole moment	Cm
q	Point charge	C
Φ	Electric potential	V
$\boldsymbol{v}$	Velocity vector	$\mathrm{m\ s^{-1}}$
v	Velocity	$\mathrm{m\ s^{-1}}$
η	Viscosity	Pa s
Q	Volume flow rate	$\mathrm{m^3\ s^{-1}}$
Ω	Computational domain	
$\partial\Omega$	Domain boundary	

1 Introduction

In this report we will study dielectric spherical objects in dielectric media. We want to analyze the dielectrophoretic force exerted on a spherical object when an external potential is applied. This will be done by giving a brief introduction of the lowest-order approximation of the dielectrophoretic force. The approximation is only valid in a limited number of problems, namely the once where the electric field is almost homogenous over the diameter of the object. We will go beyond this basic approximation and study its validity by deriving an exact expression. To derive this expression we start off by examining general force calculation on dielectric bodies in dielectric media. The result obtained by these studies will be the starting point when deriving our own expression for the dielectrophoretic force.

When deriving the expression for the dielectrophoretic force we consider a spherical object with no free charge. We can therefore start out by solving Laplace's equation to get the potential inside and outside the dielectric sphere. When solving Laplace's equation, we restrain ourselves to azimuthal symmetric external potentials as the general solution for an asymmetric potential has proven very hard to deal with. From the potentials obtained, the bound surface charge density on the sphere is found using that the perpendicular component of $\mathbf{E}$ is not continuous across a charged boundary. With the surface charge density determined the force can be calculated, since only the external field will exert a net force on the sphere. From these results and a lot of algebra our exact expression, which will end up as an infinite sum, follows.

The expression derived will be tested against the lowest-order approximation for different simple fields, which can be handled analytically. It is seen that our expression will contain the lowest-order approximation as the lowest nonzero term of the sum. Furthermore it will yield all the expected results for a dielectrophoretic force like positive and negative dielectrophoresis.

Further our result will be developed to handle spherical objects of more than one shell with different permittivities. This result is of interest when developing models for biological cells as they contain many different parts of varying electric characteristics. We also develop our expression to be valid when an AC voltage is used as the external field. A lot of the theory from DC can be reused, and the development into AC is very reasonable, as for example Debye layer forming at the electrodes in conducting fluids can be avoided. Furthermore critical frequencies for changes in the sign of the dielectrophoretic force will arise, which yields positive and negative dielectrophoretic forces dependent on frequencies.

We will also give an example that shows the scope of knowing the exact dielectrophoretic force from an asymmetric potential. We namely see a lot of possibilities in continuous separation of dielectric spheres in a microchannel. This is done in one very artificial setup, but it shows the advantages of having the full expression at disposal, so al different kinds of setups could be investigated.

At the end we will sketch the problem of finding the expression for asymmetric potentials and motivate the possibility of actually finding a solution.

2 The lowest-order approximation of the dielectrophoretic force

We consider a sphere of radius a made of a non-conducting, isotropic, homogeneous and linear dielectric[1] with permittivity ϵ_1. The sphere is placed in a dielectric medium with permittivity ϵ_2. If a nonuniform electric field is applied, the sphere will be polarized and experience a dielectrophoretic (DEP) force.

The lowest-order approximation of the DEP force is based on the following considerations. If we place a dielectric sphere in an uniform electric field $\mathbf{E}_0$, a distribution of bound charge will be induced on the surface of the sphere. Since we consider a homogeneous linear dielectric the bound volume charge density will be proportional to the free volume charge density, and hence zero. The bound surface charge will give rise to an induced electric field. A well known result from electrostatics is that the induced electric field outside the sphere is that of a pure dipole, where the dipole moment is given by [1]

$$\mathbf{p} = 4\pi\epsilon_2 \frac{\epsilon_1 - \epsilon_2}{\epsilon_1 + 2\epsilon_2} a^3 \mathbf{E}_0. \tag{1}$$

In general the force on a dipole is $\mathbf{F} = (\mathbf{p} \cdot \boldsymbol{\nabla})\mathbf{E}$, where $\mathbf{E}$ refers to the applied field. Assuming that $\mathbf{E}$ does not vary significantly over the diameter of the sphere, it is only necessary to use the first term of a Taylor expansion of the electric field, when determining the dipole moment and the force. The lowest-order approximation of the DEP force is then given by [1]

$$\mathbf{F}_{\mathrm{DEP}}^{\mathrm{app}}(\mathbf{r}_0) = 2\pi\epsilon_2 K(\epsilon_1, \epsilon_2) a^3 \boldsymbol{\nabla} \left[\mathbf{E}(\mathbf{r}_0)^2\right], \tag{2}$$

where $\mathbf{r}_0$ is the center coordinate of the sphere and $K(\epsilon_1, \epsilon_2)$ is the Clausius-Mossotti factor

$$K(\epsilon_1, \epsilon_2) = \frac{\epsilon_1 - \epsilon_2}{\epsilon_1 + 2\epsilon_2}. \tag{3}$$

If the requirement for the variation of the electric field is not met, one would expect Eq. (2) to break down because it simply neglects contributions from higher-order poles, which will be induced, if the particle is placed in a non uniform electric field.

[1] From now on the dielectrics considered are always assumed to be non-conducting, isotropic, homogeneous and linear if not specified otherwise.

3 Force on a dielectric object in a dielectric medium

In the following we will give a brief discussion of the force calculations in dielectrics. This topic is discussed in detail in [2]. We will verify that the right way to calculate the force on a dielectric object with a total distribution of charge, ρ_t, placed in a dielectric medium with relative permittivity ϵ_r is

$$\mathbf{F} = \epsilon_r \int \rho_t \mathbf{E} \mathrm{d}\tau. \tag{4}$$

$\mathbf{E}$ refers to the total electric field and $\rho_t = \rho_f + \rho_b$ includes both free and bound charge densities.

To verify Eq. (4) we first assume space filled completely with a linear isotropic dielectric material. In this case the following equations hold

$$\begin{aligned} \mathbf{P} &= \epsilon_0 \chi_e \mathbf{E}, & (5)\\ \epsilon_r &= \frac{\epsilon}{\epsilon_0} = 1 + \chi_e, & (6) \end{aligned}$$

where χ_e denotes the electric susceptibility. From Maxwell's equations we have

$$\boldsymbol{\nabla} \cdot \mathbf{E} = \frac{\rho_t}{\epsilon_0}. \tag{7}$$

Like in Eq. (4) $\rho_t = \rho_f + \rho_b$ is the total volume charge density, ρ_f is the free charge density and ρ_b denotes the bound charge density, which is given by $\rho_b = -\boldsymbol{\nabla} \cdot \mathbf{P}$. Eq. (7) can therefore be rewritten as

$$\begin{aligned} \epsilon_0 \left[\boldsymbol{\nabla} \cdot \mathbf{E}\right] &= \rho_f - \boldsymbol{\nabla} \cdot \mathbf{P} & (8)\\ &= \rho_f - \epsilon_0 \boldsymbol{\nabla} \cdot (\chi_e \mathbf{E}) & (9)\\ &= \rho_f - \epsilon_0 \chi_e \boldsymbol{\nabla} \cdot \mathbf{E} - \epsilon_0 \mathbf{E} \cdot \boldsymbol{\nabla} \chi_e, & (10) \end{aligned}$$

or

$$\epsilon_0 \left[\boldsymbol{\nabla} \cdot \mathbf{E}\right](1 + \chi_e) = \rho_f - \epsilon_0 \mathbf{E} \cdot \boldsymbol{\nabla} \chi_e. \tag{11}$$

Using the fact that

$$\boldsymbol{\nabla} \chi_e = \boldsymbol{\nabla}(1 + \chi_e) = \boldsymbol{\nabla} \epsilon_r, \tag{12}$$

and inserting Eqs. (6) and (7) into Eq. (11) it follows that

$$\rho_t \epsilon_r = \rho_f - \epsilon_0 \mathbf{E} \cdot \boldsymbol{\nabla} \epsilon_r. \tag{13}$$

Thus we see, that if $\boldsymbol{\nabla} \epsilon_r = 0$ everywhere, the total and the free charge densities are related in the following way

$$\rho_t \epsilon_r = \rho_f. \tag{14}$$

By means of energy considerations it can be deduced that the total force on a dielectric body immersed in a dielectric medium and subject to a total electric field is [2]

$$\mathbf{F} = \int_\Omega \left(\rho_f \mathbf{E} - \epsilon_0 \frac{E^2}{2} \boldsymbol{\nabla} \epsilon_r \right) \mathrm{d}\tau, \tag{15}$$

Here ϵ_r is the relative permittivity of the body and Ω is its volume. For Eq. (15) to describe the total force on the body it must also include the contribution of surface charge densities. We then have to

make the assumption that the boundary consists of a transition layer of actual spatial extension, δ, different from zero, so that the contribution from the boundary can be included in the volume integral Eq. (15). In this transition layer the permittivity varies rapidly but still continuous. If we let δ tend to zero a discontinuity is created and the gradient of the permittivity is not defined. In this case we can not use Eq. (15) as it stands. To avoid this problem we have to use some physical insight.

We therefore consider an object, A, with relative permittivity, ϵ_{r_A}, immersed in a dielectric fluid with relative permittivity ϵ_r. The object has a total amount of bound and free charge densities, $\rho_{t_A} = \rho_{f_A} + \rho_{b_A}$. In this case the permittivity has a discontinuity at the interface between the two dielectrics and the gradient in Eq. (15) is not defined.

Instead we now consider an equivalent problem, where an object B of the same size and shape as object A, but with relative permittivity ϵ_r, is placed in the fluid. Object B is subject to the same external field and it is assumed to have a total amount of frozen in charge, so that $\rho_{t_B} = \rho_{f_B} + \rho_{b_B} = \rho_{t_A}$. As the two problems have the same total charge densities and the same external field is applied, the forces $\mathbf{F}_A$ and $\mathbf{F}_B$ must be the same. In the modified problem we see, that the gradient of the relative permittivity vanishes and Eq. (15) yields the force

$$\mathbf{F}_A = \mathbf{F}_B = \int \rho_{f_B} \mathbf{E} \mathrm{d}\tau = \epsilon_r \int \rho_{t_B} \mathbf{E} \mathrm{d}\tau = \epsilon_r \int \rho_{t_A} \mathbf{E} \mathrm{d}\tau, \tag{16}$$

where we have used Eq. (14). From this result Eq. (4) follows directly.

4 The exact DEP force in an azimuthal symmetric potential

To analyze the validity of the lowest-order approximation of the DEP force we need to compare Eq. (2) to an exact expression. However we have not been able to find such an expression. We will therefore derive one ourselves.

A dielectric sphere is placed at the origin in a dielectric fluid and an external potential is applied. We assume that the sources of the external potential are placed outside the region of interest, by which we mean some area around the sphere. Since there will be no free volume charge we solve Laplace's equation,

$$\nabla^2 \Phi = 0, \tag{17}$$

to determine the potential in the region of interest. The general solution of Laplace's equation under asymmetric conditions turns out to be cumbersome to deal with when deriving an exact expression of the DEP force. Therefore we will instead consider azimuthal symmetric potentials and briefly discuss the problem involving asymmetric potentials in a later section.

4.1 The general solution of Laplace's equation

Since we consider a sphere placed at the origin, it is natural to work in spherical coordinates. If azimuthal symmetry is present the general solution of Laplace's equation is given by [3]

$$\Phi(r,\theta) = \sum_{n=0}^{\infty} \left(A_n r^n + \frac{B_n}{r^{n+1}} \right) P_n(\cos\theta), \tag{18}$$

where $P_n(x)$ is a Legendre polynomial of the order n defined by Rodrigues formula,

$$P_n(x) = \frac{1}{2^n n!} \left(\frac{\mathrm{d}}{\mathrm{d}x} \right)^n \left(x^2 - 1 \right)^n. \tag{19}$$

The Legendre polynomials are orthogonal functions and they obey

$$\int_{-1}^{1} P_n(x) P_{n'}(x) \mathrm{d}x = \begin{cases} 0, & \text{if } n' \neq n, \\ \frac{2}{2n+1}, & \text{if } n' = n, \end{cases} \tag{20}$$

$$\int_{-1}^{1} x P_n(x) P_{n'}(x) \mathrm{d}x = \begin{cases} \frac{2(n+1)}{(2n+1)(2n+3)}, & \text{for } n' = n+1, \\ \frac{2n}{(2n-1)(2n+1)}, & \text{for } n' = n-1, \\ 0, & \text{otherwise.} \end{cases} \tag{21}$$

The derivative of a Legendre polynomial of the order n is given by

$$\frac{\mathrm{d}}{\mathrm{d}x} P_n(x) = P'(x) = \frac{(n+1)P_{n+1}(x) - x(n+1)P_n(x)}{x^2 - 1}. \tag{22}$$

These properties of the Legendre polynomials have been found at [4].

4.2 The solution of Laplace's equation in the azimuthal symmetric case

As mentioned we assume that no charges are present in the region of interest, i.e. in the region where Laplace's equation has to be solved. Therefore the externally applied potential can only be of the form

$$\Phi_{\text{ext}}(r,\theta) = \sum_{n=0}^{\infty} A_n r^n P_n(\cos\theta), \tag{23}$$

where A_n is assumed known and $B_n = 0$ for all n to avoid the potential from blowing up at the origin, which would indicate the presence of charge there.

Next we place a dielectric sphere of radius a at the origin, see Fig. 1. The permittivity of the sphere is ϵ_1 and that of the surrounding media is ϵ_2.

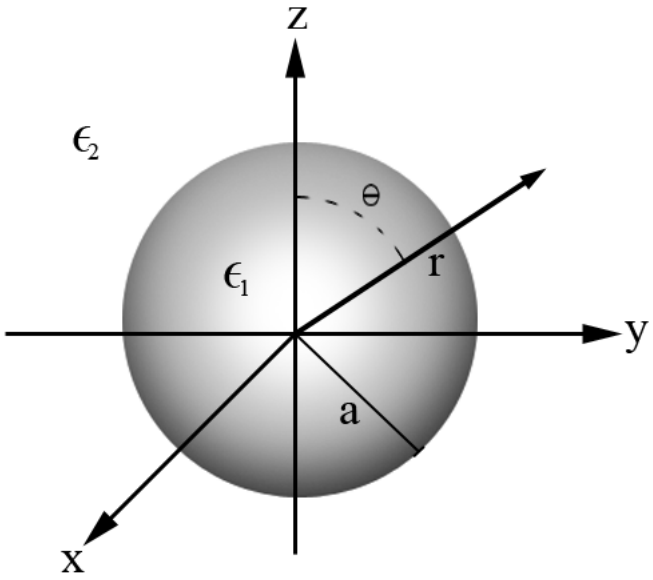

Figure 1: A dielectric sphere of radius a and with permittivity ϵ_1 placed at the origin in a dielectric medium with permittivity ϵ_2.

The external potential will result in an accumulation of bound surface charge at the interface between the sphere and the surrounding medium. The bound surface charge is due to polarization and gives rise to an induced potential inside and outside the sphere.

The potential inside the sphere is given by the external and an induced contribution. Neither of these is allowed to blow up at the origin and the total potential must therefore be of the form

$$\Phi_{\text{in}}(r,\theta) = \sum_{n=0}^{\infty} C_n r^n P_n(\cos\theta). \tag{24}$$

Outside the sphere the induced potential must tend to zero as r approaches infinity and only Φ_{ext} survives. The total potential outside the sphere is therefore of the form

$$\Phi_{\text{out}}(r,\theta) = \Phi_{\text{ext}}(r,\theta) + \sum_{n=0}^{\infty} \frac{D_n}{r^{n+1}} P_n(\cos\theta) \tag{25}$$

$$= \sum_{n=0}^{\infty} \left(A_n r^n + \frac{D_n}{r^{n+1}} \right) P_n(\cos\theta). \tag{26}$$

To determine C_n and D_n we apply the following boundary conditions

$$\Phi_{\text{in}}(a,\theta) = \Phi_{\text{out}}(a,\theta), \tag{27}$$

$$\epsilon_1 \frac{\partial}{\partial r} \Phi_{\text{in}}(r,\theta)\Big|_{r=a} = \epsilon_2 \frac{\partial}{\partial r} \Phi_{\text{out}}(r,\theta)\Big|_{r=a}. \tag{28}$$

The boundary condition Eq. (27) is due to the fact that the potential is continuous across any boundary. Eq. (28) is applied because no free charge is present at the interface between the sphere and the fluid, which makes the perpendicular component of **D** continuous. Combining Eqs. (24), (26) and (27) we get

$$\sum_{n=0}^{\infty} C_n a^n P_n(\cos\theta) = \sum_{n=0}^{\infty} \left(A_n a^n + \frac{D_n}{a^{n+1}} \right) P_n(\cos\theta). \tag{29}$$

When multiplying with $P_m(\cos\theta)\sin\theta$ and integrating with respect to θ from 0 to π, we have

$$\sum_{n=0}^{\infty} C_n a^n \int_0^{\pi} P_n(\cos\theta) P_m(\cos\theta) \sin\theta \mathrm{d}\theta =$$
$$\sum_{n=0}^{\infty} \left(A_n a^n + \frac{D_n}{a^{n+1}} \right) \int_0^{\pi} P_n(\cos\theta) P_m(\cos\theta) \sin\theta \mathrm{d}\theta. \tag{30}$$

The substitution $x = \cos\theta$ yields

$$\sum_{n=0}^{\infty} C_n a^n \int_{-1}^{1} P_n(x) P_m(x) \mathrm{d}x = \sum_{n=0}^{\infty} \left(A_n a^n + \frac{D_n}{a^{n+1}} \right) \int_{-1}^{1} P_n(x) P_m(x) \mathrm{d}x. \tag{31}$$

Using the relation Eq. (20) we arrive at

$$C_m a^m = A_m a^m + \frac{D_m}{a^{m+1}}. \tag{32}$$

The last three steps will from now on be referred to as using the orthogonality.

Combining Eqs. (24), (26) and (28) we get

$$\epsilon_1 \sum_{n=0}^{\infty} n C_n a^{n-1} P_n(\cos\theta) = \epsilon_2 \sum_{n=0}^{\infty} \left(n A_n a^{n-1} - (n+1) \frac{D_n}{a^{n+2}} \right) P_n(\cos\theta). \tag{33}$$

Using the orthogonality this reduces to

$$\epsilon_1 m C_m a^{m-1} = \epsilon_2 \left(m A_m a^{m-1} - (m+1) \frac{D_m}{a^{m+2}} \right). \tag{34}$$

Solving Eqs. (32) and (34) with respect to the unknowns C_m and D_m we get

$$C_m = \frac{(2m+1)\epsilon_2}{\epsilon_2(m+1) + \epsilon_1 m} A_m, \tag{35}$$

$$D_m = \frac{m(\epsilon_2 - \epsilon_1) a^{2m+1}}{\epsilon_2(m+1) + \epsilon_1 m} A_m. \tag{36}$$

Since A_n is assumed known, C_n and D_n are now determined and the solution to Laplace's equation inside and outside the sphere is

$$\Phi_{\mathrm{in}}(r,\theta) = \sum_{n=0}^{\infty} \frac{(2n+1)\epsilon_2}{\epsilon_2(n+1) + \epsilon_1 n} A_n r^n P_n(\cos\theta), \tag{37}$$

$$\Phi_{\mathrm{out}}(r,\theta) = \sum_{n=0}^{\infty} A_n r^n P_n(\cos\theta) + \sum_{n=0}^{\infty} \frac{n(\epsilon_2 - \epsilon_1)}{\epsilon_2(n+1) + \epsilon_1 n} \frac{a^{2n+1}}{r^{n+1}} A_n P_n(\cos\theta). \tag{38}$$

The induced potential outside the sphere can then be identified as

$$\Phi_{\text{ind}}(r,\theta) = \sum_{n=0}^{\infty} \frac{n(\epsilon_2-\epsilon_1)}{\epsilon_2(n+1)+\epsilon_1 n} \frac{a^{2n+1}}{r^{n+1}} A_n P_n(\cos\theta) \tag{39}$$

$$= -\sum_{n=0}^{\infty} K_n \frac{a^{2n+1}}{r^{n+1}} A_n P_n(\cos\theta), \tag{40}$$

where K_n is the higher-order Clausius-Mossotti factor defined by

$$K_n \equiv \frac{n(\epsilon_1-\epsilon_2)}{\epsilon_1 n+\epsilon_2(n+1)}. \tag{41}$$

Note that for $n=1$, K_n reduces to the Clausius-Mossotti factor, Eq. (3). The result Eq. (40) reveals the interesting fact that field terms of order n induce poles of order $n+1$, which will treat more closely later.

Note that Eq. (40) includes the case of a dielectric sphere placed in an uniform electric field. A field of the form $\mathbf{E} = E_0\hat{\mathbf{z}}$ has the potential

$$\Phi(r,\theta) = -E_0 r\cos\theta, \tag{42}$$

in which we arbitrarily have set $\Phi(r,\theta)|_{z=0} = 0$. The potential Eq. (42) is of the form Eq. (23) and one can identify

$$A_n = \begin{cases} -E_0, & \text{for } n=1, \\ 0, & \text{for } n\neq 1. \end{cases} \tag{43}$$

Thus from Eq. (40) we get

$$\Phi_{\text{ind}}(r,\theta) = \frac{\epsilon_1-\epsilon_2}{\epsilon_1+2\epsilon_2} a^3 E_0 \frac{\cos\theta}{r^2}. \tag{44}$$

Since the potential from a dipole depends on $\cos\theta/r^2$, we see that, as expected, an uniform field induces a dipole moment in the sphere.

4.3 The bound surface charge density

To determine the electric force on the sphere Eq. (4) we need the know the total charge density. In the previous section we solved Laplace's equation, so the volume charge density will be zero everywhere and any accumulation of charge must be on the surface of the sphere. Hence we will now determine the surface charge density using the discontinuity of the perpendicular component of the electric field across a charged boundary

$$\left.\frac{\partial}{\partial r}\Phi_{\text{out}}(r,\theta)\right|_{r=a} - \left.\frac{\partial}{\partial r}\Phi_{\text{in}}(r,\theta)\right|_{r=a} = -\frac{1}{\epsilon_0}\sigma(\theta). \tag{45}$$

By the means of Eqs. (24) and (26), the surface charge density is given by

$$\sigma(\theta) = -\epsilon_0 \sum_{n=0}^{\infty} \left(n a^{n-1}(A_n - C_n) - (n+1)\frac{D_n}{a^{n+2}} \right) P_n(\cos\theta). \tag{46}$$

Inserting Eqs. (35) and (36) and using straightforward algebra one arrives at

$$\sigma(\theta) = -\epsilon_0 \sum_{n=0}^{\infty} A_n a^{n-1} \frac{(2n+1)n(\epsilon_1 - \epsilon_2)}{\epsilon_1 n + \epsilon_2(n+1)} P_n(\cos\theta)\,. \tag{47}$$

For later convenience we define the constant

$$M_n \equiv \frac{(2n+1)n(\epsilon_1 - \epsilon_2)}{\epsilon_1 n + \epsilon_2(n+1)} = (2n+1)K_n, \tag{48}$$

where K_n is the higher order Clausius-Mossotti factor. In terms of M_n the final result for the surface charge density is

$$\sigma(\theta) = -\epsilon_0 \sum_{n=0}^{\infty} A_n a^{n-1} M_n P_n(\cos\theta)\,. \tag{49}$$

From Eq. (40) we see that the n'th term of the external field induces a pole of order $n+1$ in the dielectric sphere. The n'th term of Eq. (49) therefore describes the charge distribution of the $n+1$'th induced pole. To get a picture of this we make a polar plot of the absolute values, of each of the first three terms in Eq. (49), plotted on the surface of a sphere, see Fig. (2). Positive values of Eq. (49) have been marked red and negative values have been marked blue. To imagine the three dimensional charge

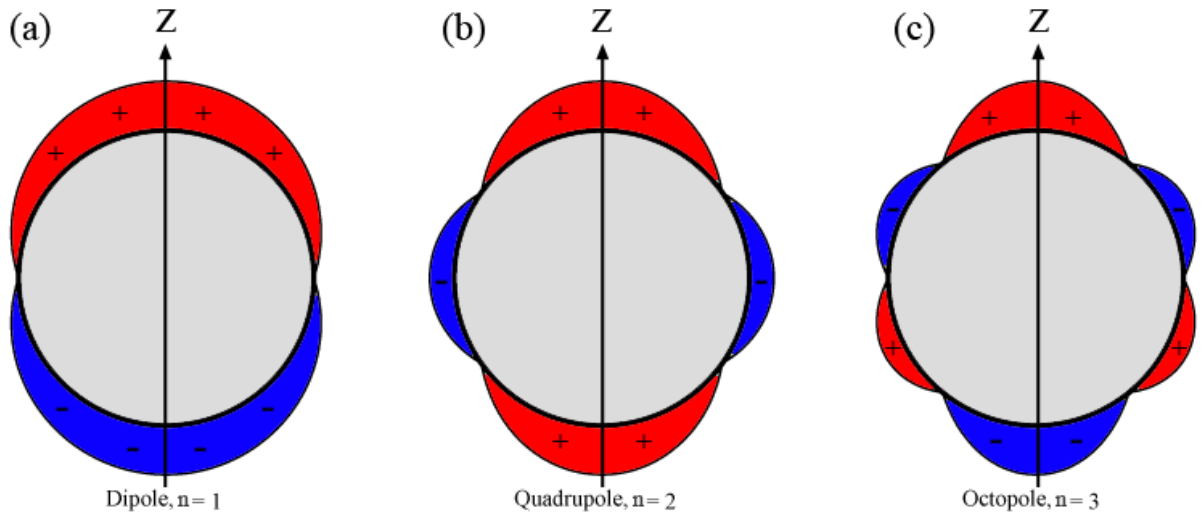

Figure 2: Surface charge distribution of the induced (a) dipole, (b) quadrupole and (c) octopole. Positive charge has been marked red and negative charge has been marked blue.

distributions one has to spin the plots around the z axis. Doing this one will realize that the dipole charge distribution, Fig. 2(a), is similar to the well-known picture of two point charges of opposite sign constituting a dipole. The charge distributions of Figs. 2(b) and 2(c) do not yield the classical images of quadrupoles and octopoles consisting of point charges, but they produce the expected potentials.

4.4 Electric force on the dielectric sphere

All the quantities needed to compute the electric force on the sphere are now known. The charge involved in our problem is located on the surface of the sphere, so Eq. (4) gives

$$\mathbf{F} = \epsilon_r \int \sigma_t \mathbf{E} \mathrm{d}a, \tag{50}$$

where $\mathbf{E}$ is the total field consisting of the externally applied field and an induced contribution. Since an infinitesimal element of surface charge, $\sigma_t \mathrm{d}a$, cannot exert a force on itself, the induced field contribution is due to all the other elements of surface charge. The exact mathematical treatment of this problem is complicated but it can be dealt with using a physical argument.

Consider another dielectric sphere of same shape and size placed in the same surroundings, but with an amount of frozen in surface charge. This surface charge is chosen so that the total charge density, free and bound, is that of the bound charge in the original problem. If no external field is applied the force on the sphere would be zero, since it cannot exert a net force on itself. If it could do so the conservation of energy would by violated, as the sphere would increase its energy without a decrease in energy in the surroundings. From this we can conclude that the net force on the original sphere due to the induced field must be zero. Hence we can replace $\mathbf{E}$ in Eq. (50) with the externally applied field.

In spherical coordinates the external field is given by

$$\begin{aligned} \mathbf{E}(r,\theta) &= -\nabla\Phi_{\mathrm{ext}}(r,\theta) && (51)\\ &= -\left(\frac{\partial}{\partial r}\Phi_{\mathrm{ext}}(r,\theta)\hat{\mathbf{r}} + \frac{1}{r}\frac{\partial}{\partial\theta}\Phi_{\mathrm{ext}}(r,\theta)\hat{\boldsymbol{\theta}} + \frac{1}{r\sin\theta}\frac{\partial}{\partial\phi}\Phi_{\mathrm{ext}}(r,\theta)\hat{\boldsymbol{\phi}}\right). && (52)\end{aligned}$$

Since the potential does not depend on ϕ the last term vanishes. The spherical unit vectors depend on position which results in a troublesome integration. Therefore we express them in cartesian coordinates

$$\begin{aligned} \mathbf{E}(r,\theta) &= -\frac{\partial}{\partial r}\Phi_{\mathrm{ext}}(r,\theta)\left(\sin\theta\cos\phi\hat{\mathbf{x}} + \sin\theta\sin\phi\hat{\mathbf{y}} + \cos\theta\hat{\mathbf{z}}\right)\\ &\quad -\frac{1}{r}\frac{\partial}{\partial\theta}\Phi_{\mathrm{ext}}(r,\theta)\left(\cos\theta\cos\phi\hat{\mathbf{x}} + \cos\theta\sin\phi\hat{\mathbf{y}} - \sin\theta\hat{\mathbf{z}}\right) && (53)\\ &= \left[-\frac{\partial}{\partial r}\Phi_{\mathrm{ext}}(r,\theta)\sin\theta - \left(\frac{1}{r}\frac{\partial}{\partial\theta}\Phi_{\mathrm{ext}}(r,\theta)\right)\cos\theta\right](\cos\phi\hat{\mathbf{x}} + \sin\phi\hat{\mathbf{y}})\\ &\quad + \left[-\frac{\partial}{\partial r}\Phi_{\mathrm{ext}}(r,\theta)\cos\theta + \left(\frac{1}{r}\frac{\partial}{\partial\theta}\Phi_{\mathrm{ext}}(r,\theta)\right)\sin\theta\right]\hat{\mathbf{z}}. && (54)\end{aligned}$$

To determine the force we integrate over the surface of the sphere with radius a

$$\mathbf{F} = \epsilon_r a^2 \int_0^{\pi}\int_0^{2\pi} \sigma(\theta)\mathbf{E}(a,\theta)\sin\theta \mathrm{d}\phi\mathrm{d}\theta. \quad (55)$$

The x and the y component vanish since integrating $\cos\phi$ and $\sin\phi$ over a 2π-period yields zero. This is to be expected due to the symmetry of the problem. As a result there will only be a net force in the z direction

$$\mathbf{F} = -2\pi\epsilon_r a^2\hat{\mathbf{z}}\left[\underbrace{\int_0^{\pi}\sigma(\theta)\left.\frac{\partial}{\partial r}\Phi_{\mathrm{ext}}(r,\theta)\right|_{r=a}\cos\theta\sin\theta\mathrm{d}\theta}_{I_1} \underbrace{-\int_0^{\pi}\sigma(\theta)\left(\frac{1}{a}\frac{\partial}{\partial\theta}\Phi_{\mathrm{ext}}(a,\theta)\right)\sin^2\theta\mathrm{d}\theta}_{I_2}\right]. \quad (56)$$

Before we evaluate the two integrals of Eq. (56) we determine the derivatives of $\Phi_{\mathrm{ext}}(r,\theta)$ Eq. (23) with respect to r and θ

$$\begin{aligned} \left.\frac{\partial}{\partial r}\Phi_{\mathrm{ext}}(r,\theta)\right|_{r=a} &= \sum_{m=0}^{\infty} mA_m a^{m-1}P_m(\cos\theta), && (57)\\ \frac{1}{a}\frac{\partial}{\partial\theta}\Phi_{\mathrm{ext}}(a,\theta) &= -\sum_{m=0}^{\infty} A_m a^{m-1}\sin\theta\left.P_m'(x)\right|_{x=\cos\theta}. && (58)\end{aligned}$$

The first integral, I_1, of Eq. (56) is evaluated in the following by means of Eqs. (49) and (57)

$$I_1 = -\epsilon_0 \int_0^\pi \left(\sum_{n=0}^{\infty} A_n a^{n-1} M_n P_n (\cos\theta) \right) \left(\sum_{m=0}^{\infty} m A_m a^{m-1} P_m (\cos\theta) \right) \cos\theta \sin\theta \mathrm{d}\theta. \tag{59}$$

Multiplying the series with one another and integrating termwise we get

$$I_1 = -\epsilon_0 \sum_{n=0}^{\infty} \sum_{m=0}^{\infty} m A_n A_m a^{n+m-2} M_n \int_0^\pi P_n (\cos\theta) P_m (\cos\theta) \cos\theta \sin\theta \mathrm{d}\theta. \tag{60}$$

Substituting $x = \cos\theta$ yields

$$I_1 = -\epsilon_0 \sum_{n=0}^{\infty} \sum_{m=0}^{\infty} m A_n A_m a^{n+m-2} M_n \int_{-1}^{1} x P_n (x) P_m (x) \mathrm{d}x. \tag{61}$$

From Eq. (21) it follows that non-zero elements will only occur if $n = m + 1$ or $m = n + 1$ and we therefore consider each of these cases. For $n = m + 1$ the non-zero elements can be described by one series, where we replace m by j

$$-\epsilon_0 \sum_{j=0}^{\infty} j A_{j+1} A_j a^{2j-1} M_{j+1} \frac{2(j+1)}{(2j+1)(2j+3)}. \tag{62}$$

For the other case where $m = n + 1$ the non-zero elements can also be described by one series, where we now replace n by j

$$-\epsilon_0 \sum_{j=0}^{\infty} (j+1) A_j A_{j+1} a^{2j-1} M_j \frac{2(j+1)}{(2j+1)(2j+3)}. \tag{63}$$

Combining the two previous equations we now have the first integral, I_1, of Eq. (56)

$$I_1 = -\epsilon_0 \sum_{j=0}^{\infty} A_j A_{j+1} a^{2j-1} \frac{2(j+1)}{(2j+1)(2j+3)} \left(j M_{j+1} + (j+1) M_j \right). \tag{64}$$

The second integral, I_2, of Eq. (56) is evaluated in the following by means of Eqs. (49) and (58)

$$I_2 = -\epsilon_0 \int_0^\pi \left(-\sum_{n=0}^{\infty} A_n a^{n-1} M_n P_n (\cos\theta) \right) \left(-\sum_{m=0}^{\infty} A_m a^{m-1} \sin\theta \left. P_m'(x) \right|_{x=\cos\theta} \right) \sin^2\theta \mathrm{d}\theta. \tag{65}$$

Again we multiply the series and integrate over each element

$$I_2 = -\epsilon_0 \sum_{n=0}^{\infty} \sum_{m=0}^{\infty} A_n A_m a^{n+m-2} M_n \int_0^\pi \sin^3\theta P_n (\cos\theta) \left. P_m'(x) \right|_{x=\cos\theta} \mathrm{d}\theta. \tag{66}$$

By the means of Eq. (22) we get

$$\begin{aligned} I_2 &= -\epsilon_0 \sum_{n=0}^{\infty}\sum_{m=0}^{\infty} A_n A_m a^{n+m-2} M_n \\ &\quad \times \int_0^{\pi} \sin^3\theta P_n(\cos\theta)\, \frac{(m+1)P_{m+1}(\cos\theta) - \cos\theta(m+1)P_m(\cos\theta)}{-\sin^2\theta} \mathrm{d}\theta \qquad (67) \\ &= \epsilon_0 \sum_{n=0}^{\infty}\sum_{m=0}^{\infty} A_n A_m a^{n+m-2} M_n (m+1) \\ &\quad \times \left(\int_0^{\pi} \sin\theta P_n(\cos\theta)\, P_{m+1}(\cos\theta)\mathrm{d}\theta - \int_0^{\pi} \sin\theta\cos\theta P_n(\cos\theta)\, P_m(\cos\theta)\mathrm{d}\theta \right) \qquad (68) \\ &= \underbrace{\epsilon_0 \sum_{n=0}^{\infty}\sum_{m=0}^{\infty} A_n A_m a^{n+m-2} M_n (m+1) \int_0^{\pi} P_n(\cos\theta)\, P_{m+1}(\cos\theta)\sin\theta \mathrm{d}\theta}_{I_{21}} \\ &\quad \underbrace{-\epsilon_0 \sum_{n=0}^{\infty}\sum_{m=0}^{\infty} A_n A_m a^{n+m-2} M_n (m+1) \int_0^{\pi} P_n(\cos\theta)\, P_m(\cos\theta)\cos\theta\sin\theta \mathrm{d}\theta}_{I_{22}} \qquad (69) \end{aligned}$$

I_2 can be separated into two double series denoted by I_{21} and I_{22}. Making the well-known substitution $x = \cos\theta$, we evaluate I_{21} which, from Eq. (20), is seen to have non-zero elements only when $n = m+1$. Replacing m by j we have

$$\begin{aligned} I_{21} &= \epsilon_0 \sum_{j=0}^{\infty} A_j A_{j+1} a^{2j-1} M_{j+1}(j+1) \frac{2}{2(j+1)+1} \qquad (70) \\ &= \epsilon_0 \sum_{j=0}^{\infty} A_j A_{j+1} a^{2j-1} \frac{2(j+1)}{(2j+1)(2j+3)} (2j+1) M_{j+1}. \qquad (71) \end{aligned}$$

The integral in I_{22} is exactly the same as that in I_1 and the double series is therefore evaluated in the same manner. I_{22} gives

$$I_{22} = -\epsilon_0 \sum_{j=0}^{\infty} A_j A_{j+1} a^{2j-1} \frac{2(j+1)}{(2j+1)(2j+3)} \left[(j+2)M_j + (j+1)M_{j+1} \right]. \qquad (72)$$

I_2 is then given by

$$\begin{aligned} I_2 &= I_{21} + I_{22} \qquad (73) \\ &= \epsilon_0 \sum_{j=0}^{\infty} A_j A_{j+1} a^{2j-1} \frac{2(j+1)}{(2j+1)(2j+3)} \left[(2j+1)M_{j+1} - (j+2)M_j - (j+1)M_{j+1} \right] \qquad (74) \\ &= \epsilon_0 \sum_{j=0}^{\infty} A_j A_{j+1} a^{2j-1} \frac{2(j+1)}{(2j+1)(2j+3)} \left[jM_{j+1} - (j+2)M_j \right]. \qquad (75) \end{aligned}$$

Inserting Eqs. (64) and (75) into Eq. (56) the dielectrophoretic force on the sphere is now determined

as

$$\begin{aligned}
\mathbf{F}_{\mathrm{DEP}} &= -2\pi\epsilon_r a^2\hat{\mathbf{z}}\,(I_1+I_2) && (76)\\
&= 2\pi\epsilon_2 a^2\hat{\mathbf{z}}\sum_{j=0}^{\infty}A_jA_{j+1}a^{2j-1}\frac{2(j+1)}{(2j+1)(2j+3)}\left[jM_{j+1}+(j+1)M_j+(j+2)M_j-jM_{j+1}\right] && (77)\\
&= 2\pi\epsilon_2 a^2\hat{\mathbf{z}}\sum_{j=0}^{\infty}A_jA_{j+1}a^{2j-1}\frac{2(j+1)}{(2j+1)(2j+3)}(2j+3)M_j && (78)\\
&= 2\pi\epsilon_2\hat{\mathbf{z}}\sum_{j=0}^{\infty}A_jA_{j+1}a^{2j+1}\frac{2(j+1)}{2j+1}M_j. && (79)
\end{aligned}$$

Inserting the constant M_j Eq. (48) in Eq. (79) the force on the sphere is finally given by

$$\mathbf{F}_{\mathrm{DEP}} = 4\pi\epsilon_2\hat{\mathbf{z}}\sum_{j=0}^{\infty}A_jA_{j+1}a^{2j+1}(j+1)\frac{j(\epsilon_1-\epsilon_2)}{\epsilon_1 j+\epsilon_2(j+1)}. \quad (80)$$

This is the exact expression for the dielectrophoretic force on the dielectric sphere when azimuthal symmetry is present. It can only be used if the source of the external field is outside the region of interest, in our case outside the sphere. This is due to the assumption of an external potential of the form Eq. (23) which is a solution to Laplace's equation.

It is worth noting that the force vanishes if $\epsilon_1 = \epsilon_2$, which is reasonable, since in this case no bound charge will be induced at the surface of the sphere.

The possibility of positive and negative dielectrophoresis is also seen from Eq. (80) as the force changes sign if either ϵ_1 or ϵ_2 has the highest value. From Eq. (80) it is not possible to determine whether $\epsilon_1 > \epsilon_2$ or $\epsilon_1 < \epsilon_2$ yields positive or negative dielectrophoresis. This is due to the fact that we can not be sure that A_j and A_{j+1} has the same sign, as they could have a dependency of $(-1)^j$ and $(-1)^{j+1}$.

The coupling between the coefficients A_j and A_{j+1} in Eq. (80) reveals some interesting physics about the interaction of the electric field terms and the multipole terms of the induced potential. The coefficients A_j can be connected to an induced pole of order $j+1$, Eq. (40), while the coefficients A_{j+1} can be connected to a field term of order $j+1$, Eq. (23). Thus Eq. (80) reveals, that only field and multipole terms of the same order can have a net force interaction. This is reasonable, since a uniform field Eq. (42), a field of order 1, induces a dipole moment in the sphere, but is not able to exert a force on it.

From the connection between A_j and the induced poles of order $j+1$, it can be interpreted that each term in the sum Eq. (80) is the force on the pole of order $j+1$ induced in the sphere, i.e. $j=1$ represents the force on the dipole moment of the sphere, $j=2$ represents the force on the quadrupole moment of the sphere, etc. This way of interpreting the terms in the sum will be useful later on.

5 The sphere in different potentials

The result for the exact DEP force Eq. (80) under azimuthal symmetric conditions shows, that the force depends on the coefficients of the external potential Eq. (23). We will therefore consider two cases where these are relatively easy to determine - the point charge potential and the dipole potential.

5.1 A point charge potential

To determine the force on the sphere from a point charge located on the z axis, see Fig. (3), one has to identify the coefficients A_j, which determine the external potential. When $r < s$ this can be done

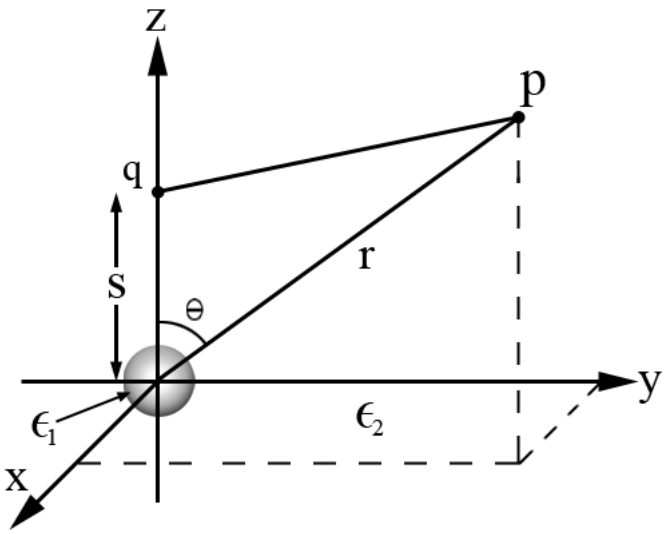

Figure 3: A point charge q is placed on the z axis from where it produces an external potential. A dielectric sphere of radius a and with permittivity ϵ_1 is placed at the origin. The permittivity of the surrounding media is ϵ_2.

by expanding the potential from the point charge in a Taylor series. This gives an expression in terms of Legendre polynomials, from which A_j can be identified. We will use this procedure for a dipole potential, but for a point charge located on the z axis we refer to [3] for the result

$$\Phi_{\rm pc}\left(r,\theta\right)=\sum_{j=0}^{\infty}A_j r^j P_j(\cos\theta),\qquad A_j=\frac{q}{4\pi\epsilon_2 s^{j+1}}. \tag{81}$$

If a dielectric sphere with radius a is present at the origin then the DEP force will be given by Eq. (80) combined with A_j from Eq. (81)

$$\mathbf{F}_{\rm DEP}=\frac{q^2}{4\pi\epsilon_2}\hat{\mathbf{z}}\sum_{j=0}^{\infty}\frac{a^{2j+1}}{s^{2j+3}}\frac{j(j+1)(\epsilon_1-\epsilon_2)}{\epsilon_1 j+\epsilon_2(j+1)}. \tag{82}$$

The first nonzero term in this sum is given by

$$\mathbf{F}_{\rm DEP}^{j=1}=\frac{q^2}{2\pi\epsilon_2}\frac{a^3}{s^5}\frac{\epsilon_1-\epsilon_2}{\epsilon_1+2\epsilon_2}\hat{\mathbf{z}}. \tag{83}$$

The potential of the point charge could also be expressed in cartesian coordinates

$$\Phi_{\rm pc}(x,y,z)=\frac{1}{4\pi\epsilon_2}\frac{q}{\sqrt{x^2+y^2+(z-s)^2}}, \tag{84}$$

which is easier to handle, when we want to use the lowest-order approximation of the DEP force, Eq. (2). To determine this approximation we now calculate $\boldsymbol{\nabla}\left[\mathbf{E}_0(\mathbf{0})^2\right]$ in the following way

$$\boldsymbol{\nabla}\left[\mathbf{E}_0(\mathbf{0})^2\right] = \left(\boldsymbol{\nabla}\left[\left(\frac{\partial\Phi_{\mathrm{pc}}}{\partial x}\right)^2+\left(\frac{\partial\Phi_{\mathrm{pc}}}{\partial y}\right)^2+\left(\frac{\partial\Phi_{\mathrm{pc}}}{\partial z}\right)^2\right]\right)\Bigg|_{(x,y,z)=\mathbf{0}}. \tag{85}$$

By straightforward algebra one gets

$$\nabla\left[\mathbf{E}(\mathbf{0})^2\right] = \frac{1}{4\pi^2\epsilon_2^2}\frac{q^2}{s^5}\hat{\mathbf{z}}, \tag{86}$$

and the lowest-order approximation of the DEP force, Eq. (2), yields the result

$$\mathbf{F}^{\mathrm{app}}_{\mathrm{DEP}}(\mathbf{0}) = \frac{q^2}{2\pi\epsilon_2}\frac{a^3}{s^5}\frac{\epsilon_1-\epsilon_2}{\epsilon_1+2\epsilon_2}\hat{\mathbf{z}}. \tag{87}$$

We see that the lowest-order approximation of the DEP force is equal to the first non zero term of the exact DEP force Eq. (83). For each term $j > 1$ Eq. (82) yields a more precise result than the lowest-order approximation. Furthermore this result supports the interpretation that the n'th term in Eq. (80) represents the force on the $n+1$'th multipole moment.

5.2 A dipole potential

We now consider the potential of a pure dipole and again we will compare the lowest-order approximation and the exact result of the DEP force. Since this requires azimuthal symmetry, we consider the problem where a pure dipole is placed on and parallel to the z axis, see Fig. 4. In this problem

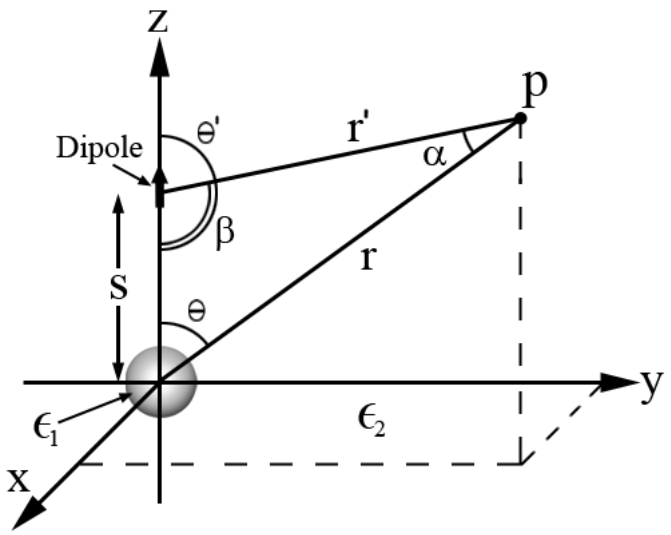

Figure 4: A pure dipole p is placed on the z axis from where it gives rise to an external potential. A dielectric sphere of permittivity ϵ_1 and radius a is placed at the origin in a dielectric media of permittivity ϵ_2.

the external potential from the dipole is given by

$$\Phi_{\mathrm{dip}}\left(r',\theta'\right) = \frac{p}{4\pi\epsilon_2}\frac{\cos\theta'}{r'^2}. \tag{88}$$

Like for the monopole we can only write the potential of the dipole on the form Eq. (23) when no charge is present in the region of interest. Hence we must demand that $r < s$ and thereby we conclude, that $\theta' \in [\pi/2, \pi]$.

To proceed we must express the external potential in the known coordinates r and θ. From the law of Cosines it is seen that

$$r' = \sqrt{s^2 + r^2 - 2rs\cos\theta}. \tag{89}$$

To avoid any inverse trigonometrical functions in the expression for $\cos\theta'$ we derive it as follows. Using the law of Sines and the fact that $\sin\beta = \sin(\pi - \theta') = \sin\theta'$we obtain

$$\sin\theta' = \frac{r}{s}\sin\alpha. \tag{90}$$

Once again the law of Cosines is used

$$\cos\alpha = \frac{r^2 + r'^2 - s^2}{2rr'} = \frac{r - s\cos\theta}{\sqrt{s^2 + r^2 - 2rs\cos\theta}}, \tag{91}$$

and

$$\sin\alpha = \sin\left[\cos^{-1}\left(\frac{r - s\cos\theta}{\sqrt{s^2 + r^2 - 2rs\cos\theta}}\right)\right] = \sqrt{1 - \left(\frac{r - s\cos\theta}{\sqrt{s^2 + r^2 - 2rs\cos\theta}}\right)^2}. \tag{92}$$

Combining Eqs. (90), (92) and the fact that $\cos(\sin^{-1}(x)) = \pm\sqrt{1 - x^2}$, see appendix A, we get

$$\cos\theta' = -\sqrt{1 - \left(\frac{r}{s}\right)^2\left(1 - \frac{r^2 + s^2\cos^2\theta - 2rs\cos\theta}{r^2 + s^2 - 2rs\cos\theta}\right)}, \tag{93}$$

where we have used that $\theta' \in [\pi/2; \pi]$ and hence $\cos\theta' < 0$ for all θ'. Substituting $x = r/s$, $\mu = \cos\theta$ and inserting Eqs. (89) and (93) into Eq. (88)

$$\Phi_{\text{dip}}(x, \mu) = -\frac{p}{4\pi\epsilon_2 s^2}\frac{\sqrt{1 - x^2\left(1 - \frac{(x-\mu)^2}{1+x^2-2x\mu}\right)}}{1 + x^2 - 2x\mu}. \tag{94}$$

To express the external potential in terms of Legendre polynomials we expand it in a Taylor series about $x = 0$

$$\frac{\sqrt{1 - x^2\left(1 - \frac{(x-\mu)^2}{1+x^2-2x\mu}\right)}}{1 + x^2 - 2x\mu} = -\left(1 + 2\mu x + \frac{3}{2}\left(3\mu^2 - 1\right)x^2 + \frac{4}{2}\left(5\mu^3 - 3\mu\right)x^3 + \ldots\right) \tag{95}$$

$$= -\sum_{n=0}^{\infty}(n+1)x^n P_n(\mu). \tag{96}$$

Combining Eqs. (94) and (96) the external potential is given by

$$\Phi_{\text{dip}}(r, \theta) = \sum_{n=0}^{\infty}\frac{p(n+1)}{4\pi\epsilon_2 s^{n+2}}r^n P_n(\cos\theta) \tag{97}$$

$$= \sum_{n=0}^{\infty}A_n r^n P_n(\cos\theta), \qquad A_n = \frac{p(n+1)}{4\pi\epsilon_2 s^{n+2}}. \tag{98}$$

If a dielectric sphere with radius a is present at the origin, the force will be given by Eq. (80) combined with A_n from Eq. (98)

$$\mathbf{F}_{\mathrm{DEP}} = 2\pi\epsilon_2\hat{\mathbf{z}}\sum_{j=0}^{\infty}\frac{p(j+1)}{4\pi\epsilon_2 s^{j+2}}\frac{p(j+2)}{4\pi\epsilon_2 s^{j+3}}a^{2j+1}\frac{2j(j+1)(\epsilon_1-\epsilon_2)}{\epsilon_2(j+1)+\epsilon_1 j} \tag{99}$$

$$= \frac{p^2}{4\pi\epsilon_2}\hat{\mathbf{z}}\sum_{j=0}^{\infty}\frac{a^{2j+1}}{s^{2j+5}}\frac{j(j+1)^2(j+2)(\epsilon_1-\epsilon_2)}{\epsilon_2(j+1)+\epsilon_1 j}. \tag{100}$$

The first nonzero term in this sum is given by

$$\mathbf{F}_{\mathrm{DEP}}^{j=1} = 3a^3\frac{p^2}{\pi\epsilon_2 s^7}\frac{\epsilon_1-\epsilon_2}{\epsilon_1+2\epsilon_2}\hat{\mathbf{z}}. \tag{101}$$

To obtain the lowest-order approximation of the DEP force, we again need the potential in cartesian coordinates

$$\Phi_{\mathrm{dip}}(x,y,z) = \frac{p}{4\pi\epsilon_2}\frac{z-s}{\left(x^2+y^2+(z-s)^2\right)^{\frac{3}{2}}}, \tag{102}$$

and we calculate $\boldsymbol{\nabla}\left[\mathbf{E}_0(\mathbf{0})^2\right]$ using Eq. (85) with Φ_{dip} instead of Φ_{pc}. By straightforward algebra one gets

$$\boldsymbol{\nabla}\left[\mathbf{E}_0(\mathbf{0})^2\right] = \frac{3}{2}\frac{p^2}{s^7\pi^2\epsilon_2^2}\hat{\mathbf{z}}. \tag{103}$$

Inserting this result into Eq. (2) we get

$$\mathbf{F}_{\mathrm{DEP}}^{\mathrm{app}}(\mathbf{0}) = 2\pi\epsilon_2 a^3\frac{\epsilon_1-\epsilon_2}{\epsilon_1+2\epsilon_2}\frac{3}{2}\frac{p^2}{s^7\pi^2\epsilon_2^2}\hat{\mathbf{z}}$$

$$= 3a^3\frac{p^2}{\pi\epsilon_2 s^7}\frac{\epsilon_1-\epsilon_2}{\epsilon_1+2\epsilon_2}\hat{\mathbf{z}}. \tag{104}$$

which is exactly the same as Eq. (101). We note again that the first term in the exact expression of the DEP force is equal to $\mathbf{F}_{\mathrm{DEP}}^{\mathrm{app}}$. Furthermore we have noticed that

$$\nabla\left[\mathbf{E}_0(\mathbf{0})^2\right] = 4A_1A_2\hat{\mathbf{z}}, \tag{105}$$

holds in both examples. We have not proved this as a general result, but it would be interesting to analyze it in further detail, as this could lead to an insight regarding the following pairs of coefficients A_jA_{j+1}.

The two previous examples indicate that the coefficients A_j of an azimuthal symmetric potential can be determined by Taylor expanding the external potential, collecting terms of like order r/s and identifying the Legendre polynomials, so that the coefficients, A_j ,appear in the obtained expression.

In both examples all charge is placed on the z axis. If one considers the case where another point charge is placed away from the z axis the azimuthal symmetry is broken. Therefore it seems reasonable that a potential only can be azimuthal symmetric if it can be constructed solely from charges on the z axis. The involved charges can either be real or image charges. As an example of the use of image charge one can consider the classical image problem of a point charge and a conducting plane. The potential of this problem can be obtained by replacing the conducting plane with an image charge. We note that the requirement of azimuthal symmetry reduces the allowed charge distributions, setting up the external potential, considerably.

6 Numerical analysis of the DEP force

From the previous section we know the exact expressions for the DEP force on the sphere in the potential from either a point charge or a dipole. It is therefore possible to evaluate the error made when using the lowest-order approximation of the DEP force in these two potentials.

For a point charge and a dipole potential the terms in the exact expression for the DEP force are respectively given by, Eqs. (82) and (100)

$$b_j^{\mathrm{pc}} = \frac{q^2}{4\pi\epsilon_2}\frac{a^{2j+1}}{s^{2j+3}}\frac{j(j+1)(\epsilon_1-\epsilon_2)}{j\epsilon_1+(j+1)\epsilon_2}, \tag{106}$$

$$b_j^{\mathrm{dip}} = \frac{p^2}{4\pi\epsilon_2}\frac{a^{2j+1}}{s^{2j+5}}\frac{j(j+1)^2(j+2)(\epsilon_1-\epsilon_2)}{\epsilon_2(j+1)+\epsilon_1 j}. \tag{107}$$

The relative error involved when using the lowest-order approximation, i.e. the first nonzero term of the exact DEP force can generally be evaluated as

$$\mathrm{RelErr_x} = \frac{\sum_{j=0}^{\infty} b_j^{\mathrm{x}} - b_1^{\mathrm{x}}}{\sum_{j=0}^{\infty} b_j^{\mathrm{x}}} = 1 - \frac{b_1^{\mathrm{x}}}{\sum_{j=0}^{\infty} b_j^{\mathrm{x}}}. \tag{108}$$

In our case x denotes either pc or dip. After some algebra we get the following expressions

$$\mathrm{RelErr_{pc}} = 1 - \frac{2}{\epsilon_1+2\epsilon_2}\frac{1}{\sum_{j=0}^{\infty}\left[\left(\frac{a}{s}\right)^{2j-2}\frac{j(j+1)}{\epsilon_1 j+(j+1)\epsilon_2}\right]}, \tag{109}$$

$$\mathrm{RelErr_{dip}} = 1 - \frac{12}{\epsilon_1+2\epsilon_2}\frac{1}{\sum_{j=0}^{\infty}\left[\left(\frac{a}{s}\right)^{2j-2}\frac{j(j+1)^2(j+2)}{\epsilon_1 j+(j+1)\epsilon_2}\right]}, \tag{110}$$

and we see, that the relative error in both cases depends on the ratio a/s.

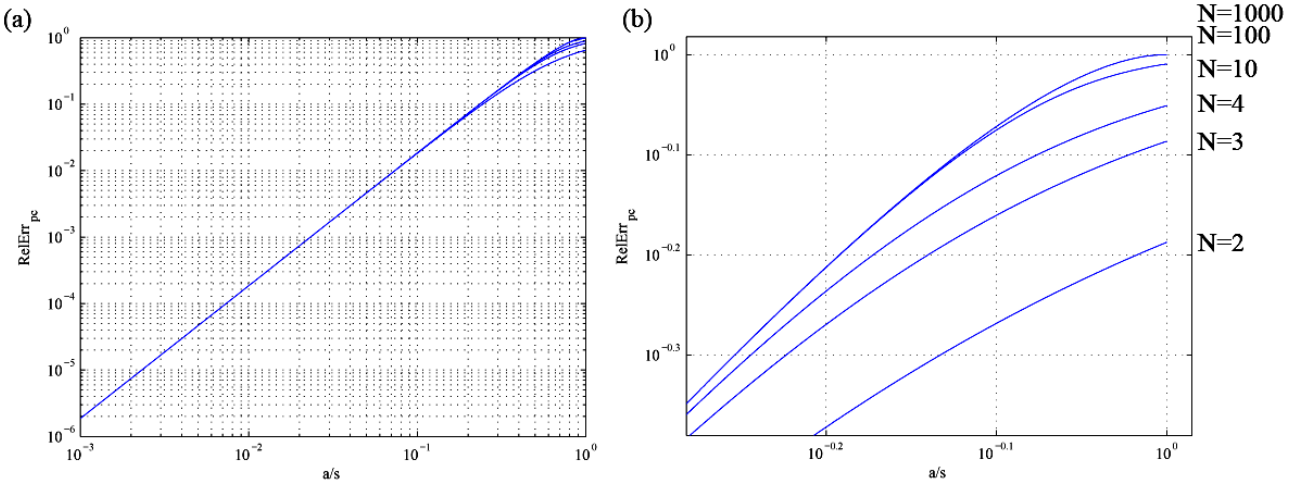

Figure 5: The relative error between the lowest-order approximation and the exact DEP force for different upper, N,limits of the sum from Eq. (109), $N = 2, 3, 4, 10, 100, 1000$ in a double logarithmic plot. (a) Plot of the relative error for $a/s \in [10^{-3}; 1]$. (b) Zoom of the relative error near $a/s = 1$. Note that the curves representing $N = 100$ and $N = 1000$ cannot be distinguished.

To analyze $\mathrm{RelErr_{pc}}$ we vary a/s and the upper limit, N, of the sum from Eq. (109). The correct plot of $\mathrm{RelErr_{pc}}$ as a function of a/s would be obtained if we could sum to infinity. As this is not possible we consider the cases where $N = 2, 3, 4, 10, 100, 1000$, see Fig. 5, which is obtained for $\epsilon_1 = 50\epsilon_0$ and

$\epsilon_2 = 80\epsilon_0$, approximately that of a cells cytoplasm and water. Note that the curves for $N = 100$ and $N = 1000$ cannot be distinguished, and therefore $N = 100$ is a good approximation to the total sum for values of a/s close to one. For a/s near zero we see that the relative error will be very small and the lowest order approximation thus valid. The reason for this is that for small values of a/s the field over the sphere will be nearly homogenous. According to section (2) this is exactly the requirement that must be fulfilled to make the lowest-order approximation of the DEP force valid.

When the sphere is moved closer to the point charge the electric field will be more and more inhomogeneous over the diameter of the sphere. As a consequence induced higher order poles will dominate and the lowest-order approximation of the DEP force will break down. This can also be seen from Fig. 5, as the relative error tends to values near one when a/s tend to one. The different behaviors of the curves for different values of N can be explained by the fact that different higher-order poles become significant at different values of a/s.

It is worth noting that the most precise graph, $N = 1000$, is a straight line in a large region, when presented in a double logarithmic plot. This means that $\mathrm{RelErr}_{\mathrm{pc}}$ can be approximated by a power function in this region.

From Eqs. (109) and (110) one would think, that the relative error also depends on the permittivities. However varying the permittivities in the range from ϵ_0 to $80\epsilon_0$ only yields minor variations of the relative error. Therefore we will leave this subject untreated.

An identical treatment of $\mathrm{RelErr}_{\mathrm{dip}}$ reveals a very similar behavior to the one just discussed for the point charge. There is only one difference in this case. It turns out that $\mathrm{RelErr}_{\mathrm{dip}}$ gives nearly coincident graphs for $N = 10$, $N = 100$ and $N = 1000$. To analyze this in further detail, we divided each of the first 21 nonzero terms in Eqs. (82) and (100) by their respective lowest-order approximations, $j = 1$. Such an analysis will namely show the dominating terms in the exact expressions. The parameters we used were $\epsilon_1 = 50\epsilon_0$, $\epsilon_2 = 80\epsilon_0$ and $a/s = 0.86, 0.75, 0.50, 0.21$, see Fig. (6).

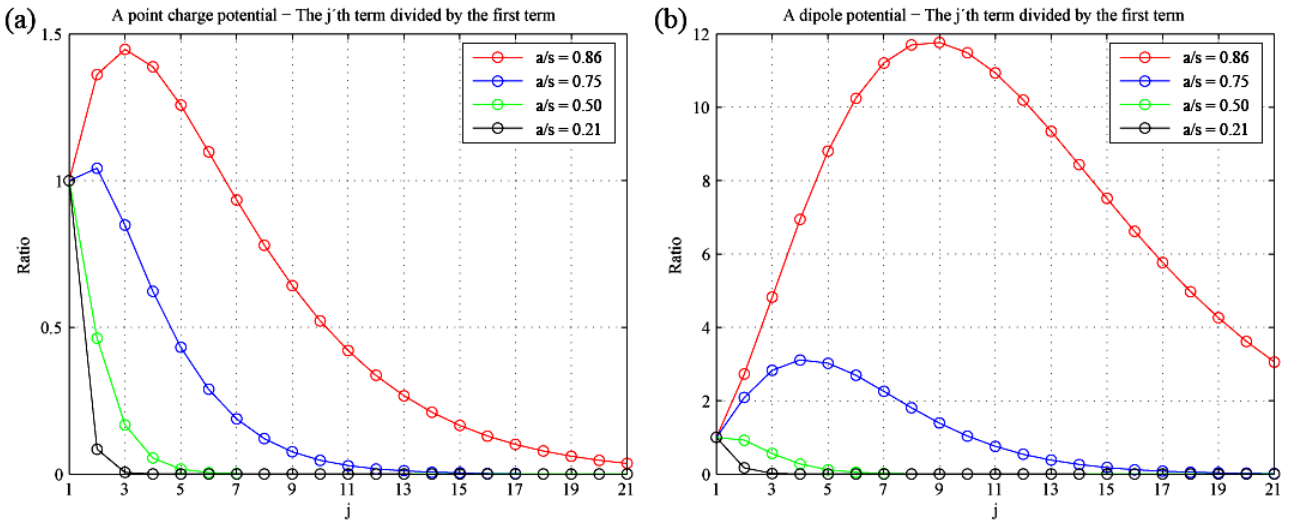

Figure 6: The plots show the first 21 nonzero terms in Eqs. (82) and (100) relative to their respective lowest-order approximations. The parameters used are $\epsilon_1 = 50\epsilon_0$, $\epsilon_2 = 80\epsilon_0$. (a) The case of a point charge potential. (b) The case of a dipole potential.

From the plots it is evident that in the cases where a/s is relatively small only the induced dipole term has a significance. We see that as the ratio a/s tends to one, induced higher-order poles become more and more dominant. Especially in Fig. 6(b) it is seen, that many higher-order poles contribute with values much larger than the first term, $j = 1$. This behavior explains why the plots for $\mathrm{RelErr}_{\mathrm{dip}}$ gives nearly coincident graphs for $N = 10$, $N = 100$ and $N = 1000$. One namely divides the first term by relatively large values in either case and Eq. (110) yields then values near one.

Finally we want to determine how many terms one need to include to make sure that the calculated force differs less than 5% from the actual value, i.e. the sum where we sum to infinity. Since this is not possible we settle when the next thousand terms satisfy the equation

$$\frac{\sum_{j=N+1}^{N+1000} b_j^{\mathrm{x}}}{\sum_{j=0}^{N} b_j^{\mathrm{x}}} \leq 0.05. \tag{111}$$

Thus it provides an estimate of the number of terms which has to be considered to get a good approximation of the DEP force. We have chosen to consider the next thousand terms as we in Fig. 6(b) have seen that the contribution from the j'th term not necessarily decreases when j increases. Once more we have considered the potentials from a point charge and a dipole. We use the values $\epsilon_1 = 50\epsilon_0$ and $\epsilon_2 = 80\epsilon_0$ and evaluate Eq. (111) as a function of a/s to obtain Fig. 7. We see that the

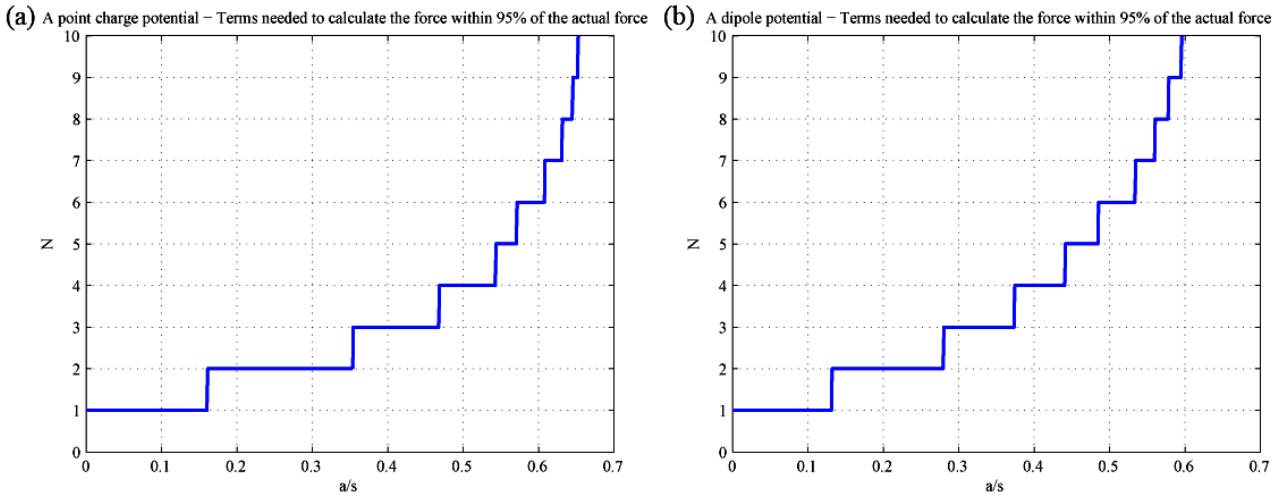

Figure 7: Plots of terms needed to calculate the force within 95% of the actual force. The plots are presented as functions of a/s. (a) The case of a point charge potential. (b) The case of a dipole potential.

lowest-order approximation of the DEP force can be considered valid only in cases where $a/s < 0.16$ for a point charge potential and $a/s < 0.13$ for a dipole potential. Furthermore it is seen that the number of terms needed, increase at lower values of a/s for the dipole potential. This is due to the potential being more non uniform over the sphere. In general one can now read the number of terms needed to calculate the force within 5% accuracy for a given value of a/s.

7 Dielectric sphere with two layers

Until now we have only considered a sphere with a homogeneous permittivity. If we want to study the behavior of a cell subject to an electric field a better model can be made. In general a biological cell consists of many different parts with different characteristics, see Fig. 8(a) for a simple example. It would be too complicated to take every part of the cell into account. Though a better, but still simple model can be obtained by considering the cell membrane as a layer with a different permittivity. Therefore we will now develop a method for handling a cell consisting of two concentric spherical shells each with different permittivity, see Fig. 8(b).

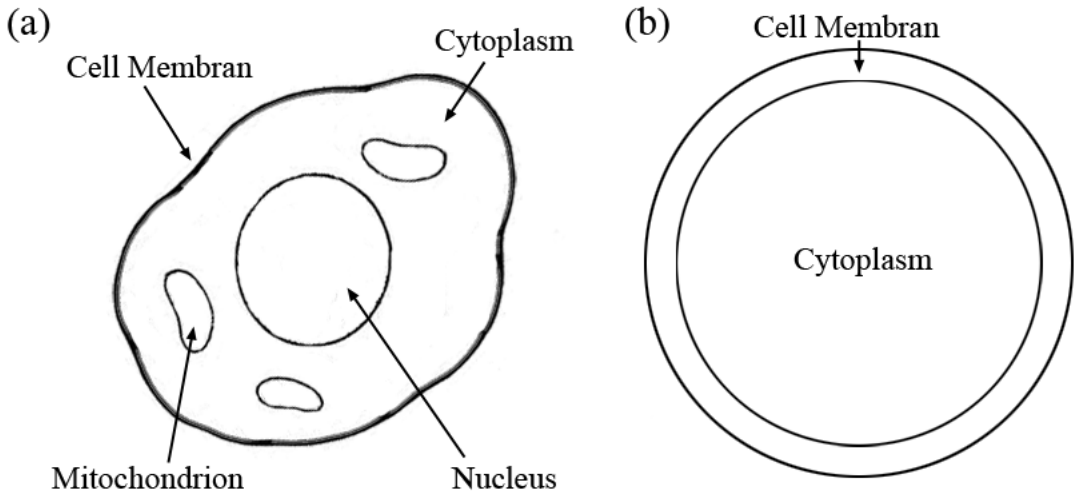

Figure 8: A comparison between a cell and a model representing it. (a) The simple biological cell. (b) The two layer model taking into account both cytoplasm and cell membrane.

For later convenience we first consider a sphere X, with permittivity, ϵ^{eff}, and of radius a_m, see Fig. 9(a). The sphere is placed in a dielectric fluid with permittivity ϵ_{m+1} and is subject to an external potential of the form Eq. (23)

$$\Phi_0(r,\theta) = \sum_{n=0}^{\infty} A_{0n} r^n P_n(\cos\theta). \tag{112}$$

From Eq. (40) it follows that the induced potential of the sphere is

$$\Phi_{\text{ind}} = -\sum_{n=0}^{\infty} K_n \frac{a_m^{2n+1}}{r^{n+1}} A_{0n} P_n(\cos\theta), \tag{113}$$

where

$$K_n = \frac{n(\epsilon^{\text{eff}} - \epsilon_{m+1})}{\epsilon^{\text{eff}} n + \epsilon_{m+1}(n+1)}. \tag{114}$$

According to the discussion above a spherical object consisting of two layers is of special interest to our studies. Assume the layers of such a sphere, X*, to have the permittivities ϵ_1 and ϵ_2 and radii a_1 and a_2 respectively, see Fig. 9(b). The surrounding fluid has the permittivity ϵ_3 and the external potential Eq. (112) is applied. Using the same arguments as in section 4.2 one may conclude that the

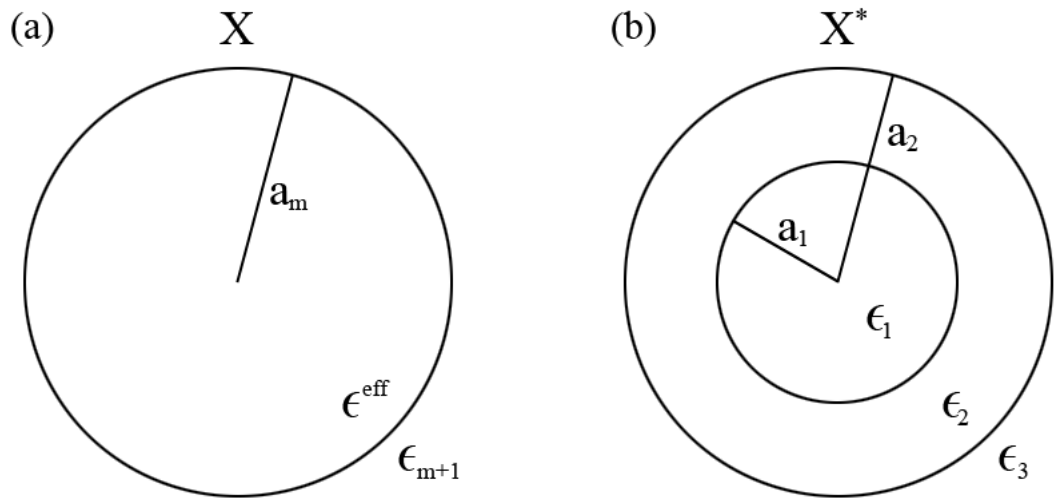

Figure 9: (a) The sphere X with radius a_m and permittivity ϵ^{eff} in a dielectric fluid of permittivity ϵ_{m+1}. (b) The two layer sphere X* with radii a_1 and a_2 and permittivities ϵ_1 and ϵ_2 in dielectric fluid of permittivity ϵ_3.

potentials in the three regions must be of the form

$$\Phi_1(r,\theta) = \sum_{n=0}^{\infty} A_{1n} r^n P_n(\cos\theta), \tag{115a}$$

$$\Phi_2(r,\theta) = \sum_{n=0}^{\infty} \left(A_{2n} r^n + \frac{B_{2n}}{r^{n+1}} \right) P_n(\cos\theta), \tag{115b}$$

$$\Phi_3(r,\theta) = \sum_{n=0}^{\infty} \left(A_{0n} r^n + \frac{B_{3n}}{r^{n+1}} \right) P_n(\cos\theta). \tag{115c}$$

The unknowns A_{1n}, A_{2n}, B_{2n}, B_{3n} have to be determined. Making use of the usual boundary conditions, Eqs. (27) and (28), we arrive at four equations with four unknowns

$$A_{1n} a_1^{2n+1} = A_{2n} a_1^{2n+1} + B_{2n}, \tag{116a}$$

$$\epsilon_1 n A_{1n} a_1^{2n+1} = \epsilon_2 \left(n A_{2n} a_1^{2n+1} - (n+1) B_{2n} \right), \tag{116b}$$

$$A_{2n} a_2^{2n+1} + B_{2n} = A_{3n} a_2^{2n+1} + B_{3n}, \tag{116c}$$

$$\epsilon_2 \left(n A_{2n} a_2^{2n+1} - (n+1) B_{2n} \right) = \epsilon_3 \left(n A_{0n} a_2^{2n+1} - B_{3n} \right). \tag{116d}$$

These four equations are easily solved using a computer. We are especially interested in the unknown B_{3n}, since it governs the total induced field outside the sphere X*. It turns out that it can be written as

$$\begin{aligned} B_{3n} &= -\frac{n\left[(\epsilon_1-\epsilon_2)(\epsilon_2(n+1)+\epsilon_3 n) a_1^{2n+1} + (\epsilon_1 n + \epsilon_2(n+1))(\epsilon_2-\epsilon_3) a_2^{2n+1}\right]}{n(n+1)(\epsilon_1-\epsilon_2)(\epsilon_2-\epsilon_3) a_1^{2n+1} + (\epsilon_1 n + \epsilon_2(n+1))(\epsilon_2 n + \epsilon_3(n+1)) a_2^{2n+1}} \\ &\quad \times a_2^{2n+1} A_{0n} \end{aligned} \tag{117}$$

The induced potential outside the sphere is then of the form

$$\Phi_{\text{ind}} = \sum_{n=0}^{\infty} \frac{B_{3n}}{r^{n+1}} P_n(\cos\theta) \tag{118}$$

Even though bound charge is accumulated at both layers of sphere X*, Eq. (118) shows, that the sphere has a net amount of induced multipole moments. It is seen that the potential due to these multipoles is of exactly the same form as Eq. (113), the potential of the single layer sphere X. This suggests that we can choose the permittivity, ϵ^{eff}, of sphere X in such a way that the induced field outside X exactly matches that of X*. Hence we can reduce the problem of a sphere consisting of two layers to a simpler problem, a sphere consisting of only one layer.

Setting $a_m = a_2$ and $\epsilon_{m+1} = \epsilon_3$ for the sphere X, it is seen that the potentials Eqs. (113) and (118) match if we set

$$K_n = -\frac{B_{3n}}{A_{0n} a_2^{2n+1}}. \tag{119}$$

This equation can be solved with respect to the permittivity of sphere X, ϵ^{eff}, and one finds

$$\begin{aligned} \epsilon_n^{\text{eff}} &= -\epsilon_2 \frac{(n+1)(\epsilon_1 - \epsilon_2) a_1^{2n+1} + (\epsilon_1 n + \epsilon_2 (n+1)) a_2^{2n+1}}{n(\epsilon_1 - \epsilon_2) a_1^{2n+1} - (\epsilon_1 n + \epsilon_2 (n+1)) a_2^{2n+1}}. & (120) \\ &= -\epsilon_2 \frac{n+1}{n} \frac{K_n \left(\frac{a_1}{a_2}\right)^{2n+1} + 1}{K_n \left(\frac{a_1}{a_2}\right)^{2n+1} - 1}, & (121) \end{aligned}$$

where K_n is the usual higher-order Clausius-Mossotti factor. As ϵ^{eff} depends on n we now denote it ϵ_n^{eff}, the effective permittivity. Since $a_1 < a_2$ we have for $n \to \infty$

$$\lim_{n \to \infty} \epsilon_n^{\text{eff}} = \epsilon_2, \tag{122}$$

which we will be of use later.

Using ϵ_n^{eff} the induced potential can then be written as

$$\Phi_{\text{ind}} = -\sum_{n=0}^{\infty} \frac{n(\epsilon_n^{\text{eff}} - \epsilon_3)}{\epsilon_n^{\text{eff}} n + \epsilon_3 (n+1)} \frac{a_2^{2n+1}}{r^{n+1}} A_{0n} P_n(\cos\theta). \tag{123}$$

As the potential is exactly the same outside the spheres X and X* they have the same induced multipolar moments. Since the force, Eq. (80), consists of the force on each of the induced multipoles it follows that the force on X and X* due to an external field must be the same. The force must therefore be given by Eq. (80) where ϵ_1 is substituted by ϵ_n^{eff} and ϵ_2 by that of the surrounding fluid ϵ_3

$$\mathbf{F}_{\text{DEP}} = 2\pi\epsilon_3 \hat{\mathbf{z}} \sum_{n=0}^{\infty} A_n A_{n+1} a_2^{2n+1} 2(n+1) \frac{n(\epsilon_n^{\text{eff}} - \epsilon_3)}{\epsilon_n^{\text{eff}} n + \epsilon_3 (n+1)}. \tag{124}$$

If we set $\epsilon_2 = \epsilon_1$ in Eq. (120) ϵ_n^{eff} reduces to ϵ_1, and Eq. (124) yields the exact same result as the force on a single layer sphere, Eq. (80).

The procedure just described can be used to find the effective permittivity of a sphere with an arbitrary number of layers, m. It is done by starting with the two innermost layers and replacing them by one layer with an effective permittivity. This procedure can then be repeated until all layers are replaced and the multilayer sphere can then be represented by a single layer sphere with a final effective permittivity. For large values of m the model could be used to approximate a sphere with a continuous varying permittivity.

7.1 Comparison of one and two layer cell models

We now wish to investigate the effect of approximating a cell by a sphere consisting of two layers instead of one. It is not possible to carry out a general analysis, where we use the parameter a/s as some of the factors in the force expression of the two layer model depends solely on a_1 or a_2. Instead we will use realistic parameters for a cell and the fluid, which it is placed in. Using these parameters we will vary the distance from the cell to a point charge, which is the source of the external potential. We use the following realistic parameters [5] $\epsilon_1 = 60\epsilon_0$, $\epsilon_2 = 65\epsilon_0$, $\epsilon_3 = 78\epsilon_0$, $a_1 = 2.5$ μm and $a_2 = 3$ μm, as given in Fig. 9(b).

Since e_n^{eff} depends on n, we cannot be sure that the ratio between each of the first 21 terms and the lowest order approximation will behave as in Fig. 6(a). We therefore have to reconsider the ratio between each of the first 21 terms and the lowest order approximation. We do this in a potential from a point charge, and use the parameters just mentioned. The result is seen in Fig. 10 and we note the great similarity to Fig. 6(a). Therefore we conclude that for the parameters chosen the behavior will be approximately the same.

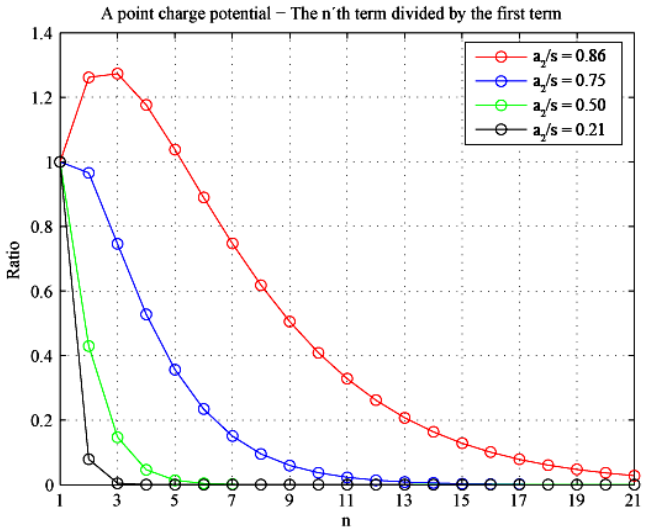

Figure 10: The plot shows the first 21 nonzero terms in Eqs. (124) relative to its lowest-order approximation. The parameters used are $\epsilon_1 = 60\epsilon_0$, $\epsilon_2 = 65\epsilon_0$, $\epsilon_3 = 78\epsilon_0$, $a_1 = 2.5$ μm and $a_2 = 3$ μm. The externally applied field is that of a point charge.

In the following we will compare the DEP force $\mathbf{F}_2$ exerted on the two layer sphere with the force $\mathbf{F}_1$ exerted on a sphere with only one layer. The one layer sphere has the the permittivity[2] ϵ_2 and radius $a = a_2 = 3$ μm.

The forces $\mathbf{F}_1$ and $\mathbf{F}_2$ are respectively given by Eq. (82) and Eq. (124) with $A_n = q/(4\pi\epsilon_2 s^{n+1})$. The ratio $|\mathbf{F_1}|/|\mathbf{F_2}|$ is plotted in Fig. 11 for different values of a_1 and 100 terms included in the DEP force sum. We used two different values of ϵ_2, $\epsilon_2 = 65\epsilon_0 > \epsilon_1 = 60\epsilon_0$, Fig. 11(a), and $\epsilon_2 = 55\epsilon_0 < \epsilon_1 = 60\epsilon_0$, Fig. 11(b).

It is seen that all graphs tend to constant values as s increases. Note that for both Figs. 11(a) and 11(b) the graph for $a_1 = 0.6$ μm reach constant values nearer the value one, than any of the other graphs. This is due to the fact that if $a_1 = 0$ μm the two layer sphere will reduce to the one layer sphere. Furthermore it is seen that as s tends to a_2 the ratio becomes one for all values of a_1. The reason for this is that when s tends to a_2, contributions due to higher-order poles will dominate, see

[2]Note that we use ϵ_2 instead of ϵ_1 as one might expect, as the cytoplasm makes up most of the cell. This is done to make the present analysis possible, and it would be reasonable for artificial particles.

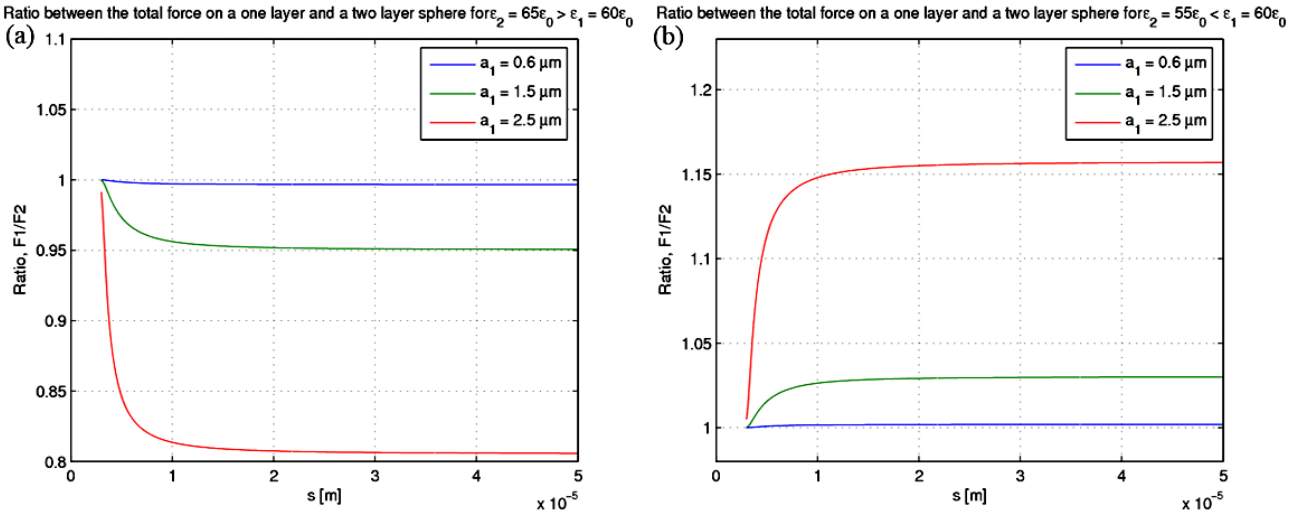

Figure 11: The ratio $|\mathbf{F_1}|/|\mathbf{F_2}|$ as a function of s for different values of a_1, the radius of the innermost sphere in the two layer sphere. In (a) $\epsilon_2 = 65\epsilon_0 > \epsilon_1 = 60\epsilon_0$ and in (b) $\epsilon_2 = 55\epsilon_0 < \epsilon_1 = 60\epsilon_0$.

Fig. 10. Since in this limit $\epsilon_n^{\text{eff}} \simeq \epsilon_2$, Eq. (122), for the higher-order contributions, the dominating terms in Eqs. (82) and (124) will be approximately equal for both the one layer and the two layer sphere.

The one big difference between the two plots is that the constant values are less than one, Fig. 11(a), or greater than one, Fig. 11(b). This means that when $\epsilon_2 > \epsilon_1$ the force on a two layer sphere will be greater than the force on a one layer sphere with permittivity ϵ_2. In the other case where $\epsilon_2 < \epsilon_1$ the force on a two layer sphere will be less than the force on a one layer sphere with permittivity ϵ_2. The reason for this can be understood from a heuristic argument like the one in [1].

We consider the two layer sphere in a fluid with the permittivity ϵ_3, which is greater than both ϵ_1 and ϵ_2. The sphere is placed in a slightly inhomogeneous electric field generated by a distribution of positive charge, see Fig. 12. In general the permittivity of a medium describes its ability to be polarized since $\mathbf{P} = (\epsilon - \epsilon_0)\mathbf{E}$, where $\mathbf{E}$ is the total electric field and the polarization $\mathbf{P}$ denotes the dipole moment per unit volume. At a boundary between two media of different permittivities and thereby polarizations an external electric field will induce a surface charge density. The reason for this is that the dipoles in each material will line up along the electric field. Since there are more dipoles "available" in one of the materials, there will be a net charge at the boundary. In the bulk of each material, however, there will be no net charge as the positive and negative ends of the dipoles cancel out.

Now we consider the case of $\epsilon_2 > \epsilon_1$, i.e. the case where the outer sphere will be polarized more than the inner sphere, see Fig. 12(a1). Let positive and negative charge cancel one to one at each surface and consider the charge left, see Fig. 12(a2). Both the dipole moment of the outer sphere and the inner sphere will point to the left. The dipole moment of the outer layer is the same as the dipole moment would be if there were no inner layer. Therefore the net dipole moment of the two layer sphere will increase compared to the one layer sphere. As the force on a dipole moment is $\mathbf{F} = (\mathbf{p} \cdot \boldsymbol{\nabla})\mathbf{E}$, the greater net dipole moment of the two layer sphere results in a greater force as seen in Fig. 11(a).

Consider the opposite case where $\epsilon_2 < \epsilon_1$, i.e. the case where the outer sphere will be polarized less than the inner sphere, see Fig. 12(b1). Let again positive and negative charge cancel one to one at each surface and consider the charge left, see Fig. 12(b2). The dipole moment of the innermost sphere will point to the right and that of the outer layer will point to the left. The dipole moment of the outer layer is the same as the dipole moment would be if there were no inner layer. Therefore the net dipole moment of the two layer sphere will decrease compared to the one layer sphere, and the force

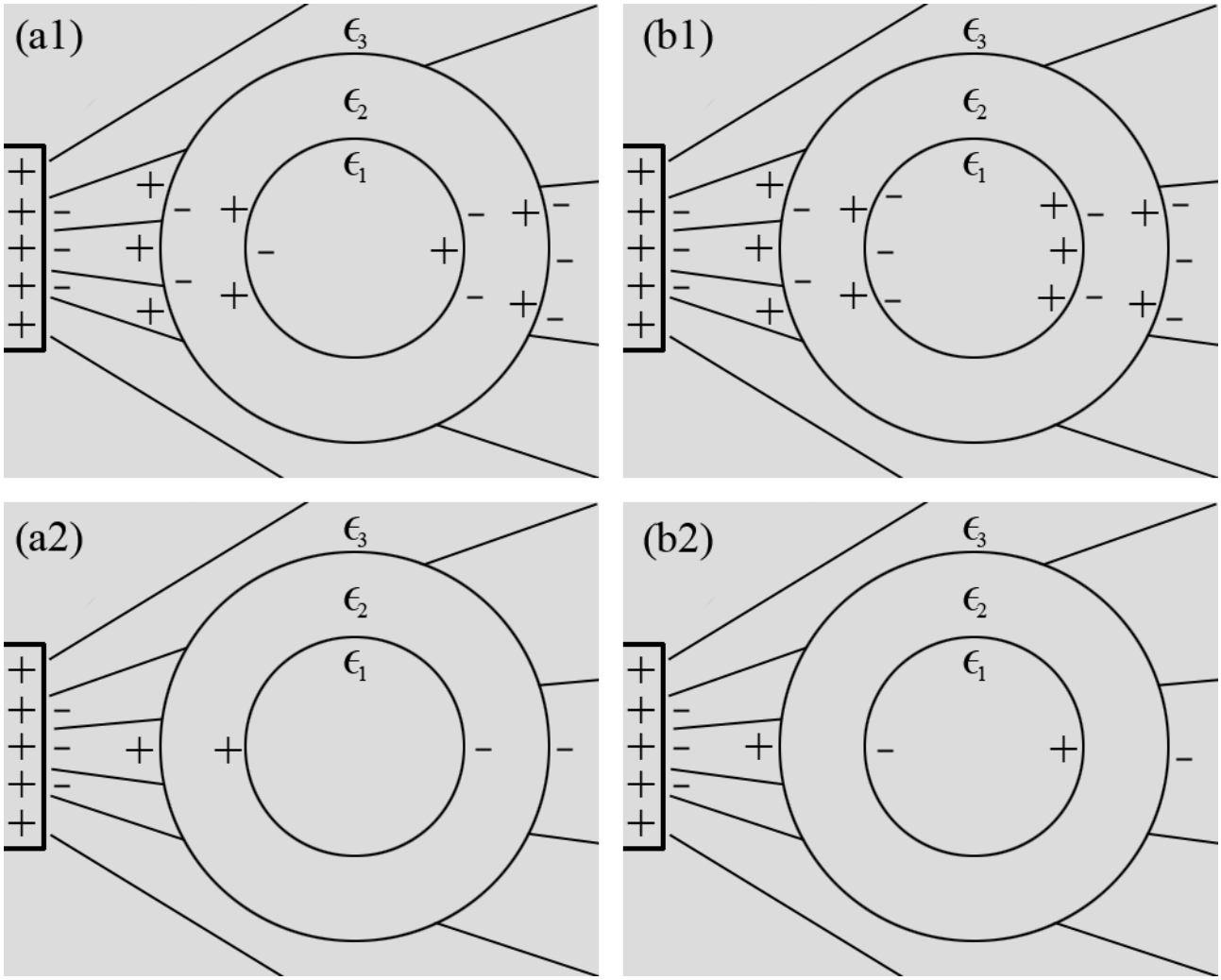

Figure 12: A two layer dielectric sphere in a fluid with the permittivity ϵ_3, which is greater than both ϵ_1 and ϵ_2. (a1) For $\epsilon_1 < \epsilon_2$ the total charge is indicated. (a2) For $\epsilon_1 < \epsilon_2$ the net charge is indicated. The inner dipole moment strengthens the overall dipole moment. (b1) For $\epsilon_1 > \epsilon_2$ the total charge is indicated. (a2) For $\epsilon_1 > \epsilon_2$ the net charge is indicated. The inner dipole moment weakens the overall dipole moment.

on the two layer sphere will also decrease, see Fig. 11(b). From this analysis we can conclude that if one desires to exert a great force on a sphere, two different cases should be considered. The first being a sphere in a fluid with a larger permittivity than the outermost layer. In this case a large force will be obtained if the permittivity of the layers decrease from the outside and in. In the second case where the fluid has a lower permittivity than the outermost layer, the permittivity has to increase from the outside and in to obtain a great force.

8 AC dielectrophoresis

We wish to approximate the force on a living cell and it is therefore necessary to consider the fluid as being conductive, since a cell will die if not present in a salt solution. The fact, that the dielectric fluid then will contain ions, causes the dielectrophoretic force to decrease in strength, as the ions will form a screening Debye layer at the electrodes. This layer will shield the electric field and thereby make dielectrophoresis impossible. To avoid the forming of a Debye layer one should therefore use AC voltage bias [1] working at an appropriate high frequency. The frequency should be chosen so that the ions do not change their mean position, to prevent the Debye layer from establishing.

The purpose of this section is to investigate the influence of the frequency on the sign of the multipole terms in the expression for the DEP force. For simplicity we will therefore only analyze the single layer sphere in an AC potential.

8.1 Electric force on the dielectric sphere subject to an AC voltage

We consider the case, where the external potential is time-dependent

$$\Phi_{\text{ext}}(r,\theta,t) = \sum_{n=0}^{\infty} A_n r^n P_n(\cos\theta)\exp(-i\omega t), \tag{125}$$

where ω denotes the frequency. Note that we have to take the real part of $\Phi_{\text{ext}}(r,\theta,t)$ to get the physical potential. The external electric field also oscillates with the frequency ω, since $\mathbf{E} = -\boldsymbol{\nabla}\Phi_{\text{ext}}(r,\theta,t)$. Furthermore the potentials induced, when a dielectric sphere is present at the origin, will also be oscillating with the frequency ω because the potential has to be continuous across the boundary for all times.

Considering the case of a sphere with one layer, we have to substitute ϵ_1 and ϵ_2 in Eq. (28) with the following relation, when dealing with AC voltage and non-zero conductivities [1]

$$\epsilon_x(\omega) = \epsilon_x - i\frac{\sigma_{el,x}}{\omega}, \quad x = 1,2, \tag{126}$$

where x denotes the medium considered. Furthermore $\sigma_{el,x}$ denotes the conductivity of the medium. With the use of this substitution the boundary conditions are equivalent to the one used in the DC-case and therefore many of the results can be reused. The constants, which determine the potentials, after the sphere is placed at the origin, are hereby easily obtained from Eqs. (35) and (36), if we make the substitutions ϵ_1 by $\epsilon_1(\omega)$ and ϵ_2 by $\epsilon_2(\omega)$. It is important to note, that only the real part of the complex constants, $\tilde{C_n}$ and $\tilde{D_n}$, should be used, when determining the time-varying surface charge density of the sphere. Using the discontinuity of the perpendicular part of the electric field we insert the real parts of $\tilde{C_n}$ and $\tilde{D_n}$ in Eq. (46) and get

$$\sigma(\theta,t) = -\epsilon_0 \sum_{n=0}^{\infty} A_n a^{n-1} N_n P_n(\cos\theta)\exp(-i\omega t), \tag{127}$$

where N_n denotes the real constant

$$N_n = \text{Re}\left[\frac{n(2n+1)(\epsilon_1(\omega)-\epsilon_2(\omega))}{\epsilon_2(\omega)(n+1)+\epsilon_1(\omega)n}\right]. \tag{128}$$

The mathematical form of $\sigma(\theta,t)$ is equivalent to Eq. (49) with $M_n = N_n\exp(-i\omega t)$. Since the time-varying electric field is $\mathbf{E}(r,\theta,t) = \mathbf{E}(r,\theta)\exp(-i\omega t)$, the force on the sphere is given by

$$\mathbf{F}(\omega,t) = \epsilon_r a^2 \exp(-i\omega t)\int_0^{\pi}\int_0^{2\pi} \sigma(\theta,t)\mathbf{E}(a,\theta)\sin\theta \mathrm{d}\phi\mathrm{d}\theta. \tag{129}$$

The double integral on the right hand side of Eq. (129) has exactly the same structure as the one we evaluated in the DC-case Eq. (55). Therefore we can use Eq. (79) with $M_n = N_n \exp(-i\omega t)$, to get the force

$$\mathbf{F}(\omega, t) = 2\pi\epsilon_2 \exp(-i\omega t)\hat{\mathbf{z}} \sum_{n=0}^{\infty} A_n A_{n+1} a^{2n+1} \frac{2(n+1)}{2n+1} N_n \exp(-i\omega t). \tag{130}$$

We want to determine the time-average of the real part of this result, but we have to be careful. In general one has to keep in mind, how the time-dependent parts of ones expression got there. This is important since

$$\mathrm{Re}\left[A(t)B(t)\right] \neq \mathrm{Re}\left[A(t)\right]\mathrm{Re}\left[B(t)\right]. \tag{131}$$

where $A(t)$ and $B(t)$ are complex functions of the form $f : R \to C$. In fact we have already dealt with a similar problem in Eqs. (127) and (128). There we chose to insert N_n as a real quantity, so that we later on would not be in doubt, whether to take the real part of a product or the product of real parts. From Eqs. (127) and (129) it is seen, that the time-dependent parts enter Eq. (130) independently so to speak, which means that we have to use the product of real parts. Hereby the time-averaging can be done using the general relation, see appendix B for the proof

$$\langle A(t)B(t)\rangle = \frac{1}{\tau}\int_0^{\tau} A(t)B(t)dt = \frac{1}{2}\mathrm{Re}\left[A_0 B_0^*\right], \tag{132}$$

where $A(t) = \mathrm{Re}\left[A_0 \exp(-i\omega t)\right]$, $B(t) = \mathrm{Re}\left[B_0 \exp(-i\omega t)\right]$ and A_0 and B_0 are complex numbers. * means the complex conjugate. Setting $A(t) = B(t) = \exp(-i\omega t)$ and making use of Eqs. (128), (130) and (132) one gets

$$\langle \mathbf{F}(\omega)\rangle = 2\pi\epsilon_2 \hat{\mathbf{z}} \sum_{n=0}^{\infty} A_n A_{n+1} a^{2n+1}(n+1)\mathrm{Re}\left[\frac{n(\epsilon_1(\omega) - \epsilon_2(\omega))}{\epsilon_2(\omega)(n+1) + \epsilon_1(\omega)n}\right], \tag{133}$$

which is very similar to Eq. (80), why the physical interpretation is the same. However there is one major difference since the real part of the complex Clausius-Mossotti factor

$$K_n(\omega) = \frac{n(\epsilon_1(\omega) - \epsilon_2(\omega))}{\epsilon_2(\omega)(n+1) + \epsilon_1(\omega)n}, \tag{134}$$

in Eq. (133) is frequency dependent. The frequency dependence will be analyzed in what follows.

8.2 The generalized critical frequency

The critical frequency for a given term of Eq. (133) is the frequency where the term changes its sign, i.e. the term of the DEP force changes its sign. This frequency can be obtained for the n'th term in Eq. (133) by demanding

$$\mathrm{Re}\left[\frac{\epsilon_1(\omega_n^c) - \epsilon_2(\omega_n^c)}{\epsilon_2(\omega_n^c)(n+1) + \epsilon_1(\omega_n^c)n}\right] = \mathrm{Re}\left[\{\epsilon_1(\omega_n^c) - \epsilon_2(\omega_n^c)\}\{\epsilon_2(\omega_n^c)(n+1) + \epsilon_1(\omega_n^c)n\}^*\right] = 0. \tag{135}$$

First of all we evaluate the complex quantity, which we want to take the real part of

$$\begin{aligned}(\epsilon_1(\omega_n^c) - \epsilon_2(\omega_n^c))\,(\epsilon_2(\omega_n^c)(n+1) + \epsilon_1(\omega_n^c)n)^* = &\left((\epsilon_1 - \epsilon_2) - \frac{i}{\omega_n^c}(\sigma_{\mathrm{el},1} - \sigma_{\mathrm{el},2})\right) \\ &\times \left((\epsilon_2(n+1) + \epsilon_1 n) + \frac{i}{\omega_n^c}(\sigma_{\mathrm{el},2}(n+1) + \sigma_{\mathrm{el},1}n)\right).\end{aligned} \tag{136}$$

The real part of this result shall equal zero, which yields

$$(\epsilon_1 - \epsilon_2)(\epsilon_2(n+1) + \epsilon_1 n) = \frac{1}{(\omega_n^{\mathrm{c}})^2} \left(\sigma_{\mathrm{el},2} - \sigma_{\mathrm{el},1}\right) \left(\sigma_{\mathrm{el},2}(n+1) + \sigma_{\mathrm{el},1} n\right), \tag{137}$$

so the critical frequency is given by

$$\omega_n^{\mathrm{c}} = \sqrt{\frac{\left(\sigma_{\mathrm{el},2} - \sigma_{\mathrm{el},1}\right) \left(\sigma_{\mathrm{el},2}(n+1) + \sigma_{\mathrm{el},1} n\right)}{(\epsilon_1 - \epsilon_2)(\epsilon_2(n+1) + \epsilon_1 n)}}, \tag{138}$$

which for $n = 1$ reduces to the critical frequency given in [1]. It is seen that the limit for $n \to \infty$ is

$$\omega_\infty^{\mathrm{c}} = \sqrt{\frac{\sigma_{\mathrm{el},2}^2 - \sigma_{\mathrm{el},1}^2}{\epsilon_1^2 - \epsilon_2^2}}. \tag{139}$$

The critical frequency depends on n and therefore every multipole term will have its own critical frequency. We have analyzed the dependency of n with the following realistic parameters for cell and fluid [5], $\sigma_1 = 0.5$ S/m, $\sigma_2 = 0.001$ S/m, $\epsilon_1 = 60\epsilon_0$ and $\epsilon_2 = 78\epsilon_0$, see Fig. 13. From Fig. 13(a) it is seen

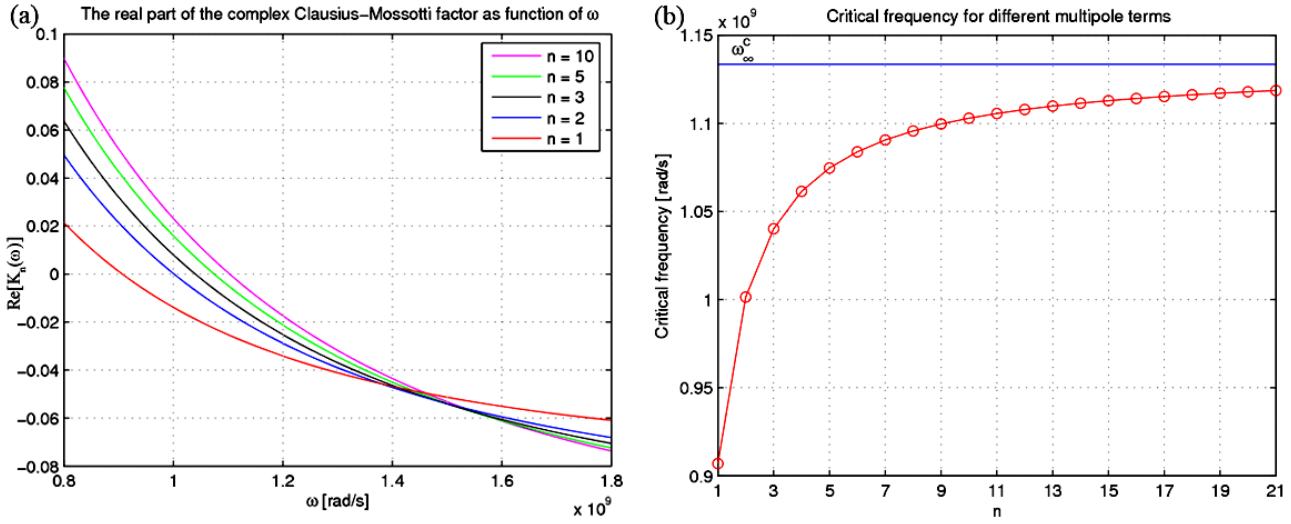

Figure 13: (a) The real part of the complex Clausius-Mossotti as a function of ω. (b) Plot of the critical frequency for the different multipole terms and the critical frequency limit $\omega_\infty^{\mathrm{c}}$. For both plots the parameters used for the cell and the fluid are $\sigma_1 = 0.5$ S/m, $\sigma_2 = 0.001$ S/m, $\epsilon_1 = 60\epsilon_0$ and $\epsilon_2 = 78\epsilon_0$

that the different orders of the real part of the complex Clausius-Mossotti factor change sign one after another when the frequency is increased. If one chooses a frequency among the critical frequencies all the orders of $\mathrm{Re}[K_n(\omega)]$ with lower critical frequencies have one sign, whereas the remaining orders will have the opposite sign.

For a given cell and fluid the critical frequencies for the different multipole terms belong to the interval $[\omega_1^{\mathrm{c}}; \omega_\infty^{\mathrm{c}}]$, see Fig. 13(b). If one choose the frequency of the AC voltage bias to be some value in this interval, it will be hard to predict the overall sign of the DEP force, if the cell is in a very inhomogeneous field. The reason for this is the changing sign of the $\mathrm{Re}[K_n(\omega)]$ and that the higher order terms will dominate the DEP force in this case, see Fig. 6. Thus one cannot be sure that ω_1^{c} will govern the sign of the DEP force, as predicted by the lowest-order approximation [1]. In general one should therefore chose the frequency of the AC voltage bias so that it does not fall within the interval $[\omega_1^{\mathrm{c}}; \omega_\infty^{\mathrm{c}}]$.

9 Simulation of sphere trajectories

So far we have derived an expression, Eq. (80), for the exact DEP force on a dielectric sphere placed in a dielectric fluid and subject to an external potential. The equation requires the external potential to be azimuthal symmetric which limits the range of problems that can be treated. If the sphere is allowed to move away from the origin in any given direction the possible potentials will be limited to only one case, the potential of a point charge. This is namely the only potential which can be made azimuthal symmetric with respect to any point in space. In practice this is done by letting a coordinate system follow the sphere and by rotating it so that the point charge always is placed on the z axis.

If the expression for the exact DEP force was not limited by azimuthal symmetry it would be possible to calculate the force acting on the dielectric sphere at any point in space and under the influence of any external potential. This would make it possible to simulate for example the trajectory of a particle flowing in a microchannel under the influence of an external electric field. To get a glimpse of the perspectives of such a simulation we will set up a very artificial though illustrative example.

To fulfill the requirements of Eq. (80) for every point in a microchannel we let a spherical electrode, which has the same potential as a point charge, set up the external potential. The electrode will be placed just inside the upper plate of an infinite parallel plate channel in which a fluid flows, see Fig. 14. The channel plates and the fluid must have the same permittivity so that the external electric field is not altered at the boundary, which would make it asymmetric. The plates could for example be made of polypropylene and the fluid could be benzene, as their permittivities nearly match, see Table 1. If two different types of spheres, with radius $a = 3$ μm, were to be sorted in the microchannel, this could be done by applying an AC potential to the electrode and utilize the spheres different critical frequencies. The interval of critical frequencies for the two spheres are given by Eq. (138) with $n = 1$ and Eq. (139)

$$\omega^{\mathrm{c}}_{\mathrm{sphere1}} : [4.707; 6.023] \times 10^{13} \mathrm{rad/s}, \tag{140}$$

$$\omega^{\mathrm{c}}_{\mathrm{sphere2}} : [7.186; 8.934] \times 10^{12} \mathrm{rad/s}, \tag{141}$$

so a frequency around 10^{13} rad/s should make sphere 1 and 2 experience forces of opposite sign.

When in a microchannel each of the spheres will be subjects to gravity, buoyancy, Stokes drag [1] and the DEP force, given by Eq. (133). In our case we choose to neglect gravity and buoyancy, as the channel could as well be upright and these forces thereby would have no effect on the trajectory, see Fig. 14.

The velocity field of the fluid is given by [1]

$$\mathbf{v}(y) = v_x(y)\hat{\mathbf{x}} = \frac{\Delta p}{2\eta L}(h - y)y\hat{\mathbf{x}}, \tag{142}$$

where $\Delta p/L$ is the pressure drop per length and η is the viscosity of the fluid. The velocity field is a parabola, so the fluid velocity will vary along the y axis, and Stokes drag will therefore only be

Material	ϵ_r	σ [$(\Omega$ m$)^{-1}$]	ρ [g cm^{-3}]	η [mPa s]
Polypropylene	2.3	-	-	-
Benzene	2.2825	10^{-14}	0.8786	0.604
Sphere 1	1.3	1000	-	-
Sphere 2	1.9	100	-	-

Table 1: Physical constants of polypropylene and benzene as given by [6] and [7]. Furthermore the values we have chosen for the spheres are also listed. These values have been chosen to illustrate positive and negative dielectrophoresis.

approximately correct in a given part of the channel. Setting $h = 100$ μm one can argue that Stokes drag will be approximately valid if $y \in [0.25; 0.75]$ μm, see appendix C.

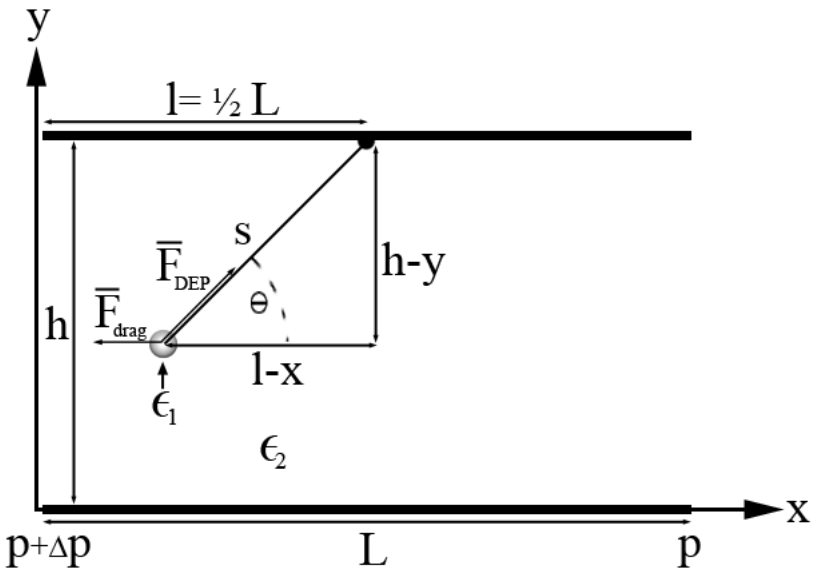

Figure 14: A dielectric sphere flowing to the right in an infinite parallel plat channel of length L and height h. The pressure drop Δp drive the Poiseuille flow. A spherical electrode sets up an external field like that of a point charge.

To determine the trajectory of the spheres we now consider Newtons second law for the sphere

$$m\mathbf{a} = \mathbf{F}_{\rm DEP} + \mathbf{F}_{\rm drag}. \tag{143}$$

The forces are given by

$$\mathbf{F}_{\rm DEP} = |\mathrm{F}_{\rm DEP}| \left(\cos\theta\hat{\mathbf{x}} + \sin\theta\hat{\mathbf{y}}\right), \tag{144}$$

$$\mathbf{F}_{\rm drag} = 6\pi\eta a \left(\mathbf{v} - \mathbf{u}\right), \tag{145}$$

where $\mathbf{F}_{\rm DEP}$ is given by Eq. (133) for an AC potential, $\mathbf{v}$ is the velocity of the fluid, if the sphere had not been there, and $\mathbf{u}$ is the velocity of the sphere. The equation of motion in the x direction is

$$\frac{d^2x}{dt^2} = \frac{|\mathrm{F}_{\rm DEP}|}{m}\cos\theta + \frac{6\pi\eta a}{m}\left(v_x(y) - \frac{dx}{dt}\right) \tag{146}$$

$$= \frac{|\mathrm{F}_{\rm DEP}|}{m}\frac{(l-x)}{\sqrt{(l-x)^2 + (h-y)^2}} + \frac{6\pi\eta a}{m}\left(v_x(y) - \frac{dx}{dt}\right), \tag{147}$$

and similarly for the y direction

$$\frac{d^2y}{dt^2} = \frac{|\mathrm{F}_{\rm DEP}|}{m}\frac{(h-y)}{\sqrt{(l-x)^2 + (h-y)^2}} - \frac{6\pi\eta a}{m}\frac{dy}{dt}. \tag{148}$$

Solving these two equations for x and y yields the trajectory of a sphere. To do this we want to use the function `ode45` in MatLab. We therefore need to rewrite the equations of motion as a system of first order differential equations. We define the vector $\mathbf{k}$ as

$$\mathbf{k} = \begin{pmatrix} k_1 \\ k_2 \\ k_3 \\ k_4 \end{pmatrix} = \begin{pmatrix} x \\ y \\ \dot{x} \\ \dot{y} \end{pmatrix}, \tag{149}$$

where a dot indicates the derivative with respect to time. The time derivative of $\mathbf{k}$ is

$$\dot{\mathbf{k}} = \begin{pmatrix} \dot{k_1} \\ \dot{k_2} \\ \dot{k_3} \\ \dot{k_4} \end{pmatrix} = \begin{pmatrix} \dot{x} \\ \dot{y} \\ \ddot{x} \\ \ddot{y} \end{pmatrix} = \begin{pmatrix} k_3 \\ k_4 \\ \frac{|\mathrm{F_{DEP}}|}{m} \frac{(l-k_1)}{\sqrt{(l-k_1)^2+(h-k_2)^2}} + \frac{6\pi\eta a}{m} \left(\frac{\Delta p}{2\eta L} (h-k_2) k_2 - k_3 \right) \\ \frac{|\mathrm{F_{DEP}}|}{m} \frac{(h-k_2)}{\sqrt{(l-k_1)^2+(h-k_2)^2}} - \frac{6\pi\eta a}{m} k_4 \end{pmatrix}. \tag{150}$$

Now the problem of solving the differential equations for $\mathbf{k}$ can be treated by Matlab's differential equations solver `ode45`, see appendix D, E and F. Finally an example of constants used in the simulation can be found in appendix G. The calculation of the constants not already mentioned will be shown in what follows.

A typical flowrate per width in a microchannel could be[3] $Q/w = 5 \cdot 10^{-7}$ m^2/s. In a infinite parallel plate channel the pressure drop is related to the flowrate per width through

$$\Delta p = \frac{12\eta L}{h^3} \frac{Q}{w}. \tag{151}$$

Setting $L = 0.122$ m and $h = 100$ μm yields $\Delta p = 495.2$ Pa. The charge on the electrode is set to around $4 \cdot 10^{-13}$ C.

The effective Reynolds number for this two length system is given by [1]

$$Re_{\mathrm{eff}} = \frac{\rho V_0 h}{\eta} \frac{h}{L}, \tag{152}$$

where $V_0 = Q/(wh)$. When calculated $Re_{\mathrm{eff}} = 0.67 \cdot 10^{-3} \ll 1$, so the flow is laminar and the assumption of Poiseuille flow is valid.

Our goal is to separate the two types of spheres and therefore we now calculate their trajectories for three different frequencies ω_1, ω_2 and ω_3, see Fig. (16). Each time the spheres start at $y = 40$ μm.

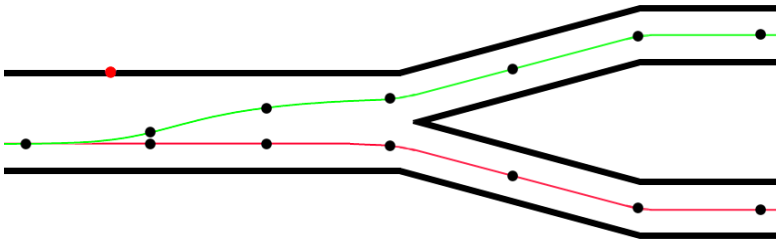

Figure 15: Imaginary design of microchannels for continuous cell separation. The electrode attracts spheres flowing along the green trajectory whereas spheres flowing along the red trajectory are sightly repelled.

$\omega_1 = 10^{12}$ rad/s is chosen, so it is under the interval of the critical frequencies for both spheres, Eqs. (140) and (141). It is seen that this choice will not sort the spheres since they both experience positive DEP and thereby are attracted towards the electrode, so they end up in the upper part of the channel. Furthermore sphere 1 crosses the validity boundary of the Stokes drag. Altogether this is a bad choice of frequency for the task at hand.

$\omega_2 = 10^{13}$ rad/s is the choice of frequency, that we would expect to solve our problem, since this frequency lies in the gab between the two intervals for the critical frequencies. From the plot it is

[3] see [1], page 52-53, Exercise 3.6

seen that this is indeed the case. Sphere 1 experience positive DEP and ends in the upper part of the channel, while sphere 2 experience negative DEP and stays in the lower part. If one imagine that the channel later on splits up in two, spheres of type 1 will end up in one channel and spheres of type 2 will end up in the other channel, see Fig. 15. Therefore ω_2 will be the right choice of frequency, if one desires to have a continuous separation of the two types of spheres.

$\omega_3 = 10^{14}$ rad/s is a frequency, that is above both intervals of critical frequencies. It is therefore expected that both spheres experience negative DEP and end up in the lower part of the channel, which is also seen from the plot. Like ω_1 this choice of frequency will not be preferable if one desires to separate the spheres.

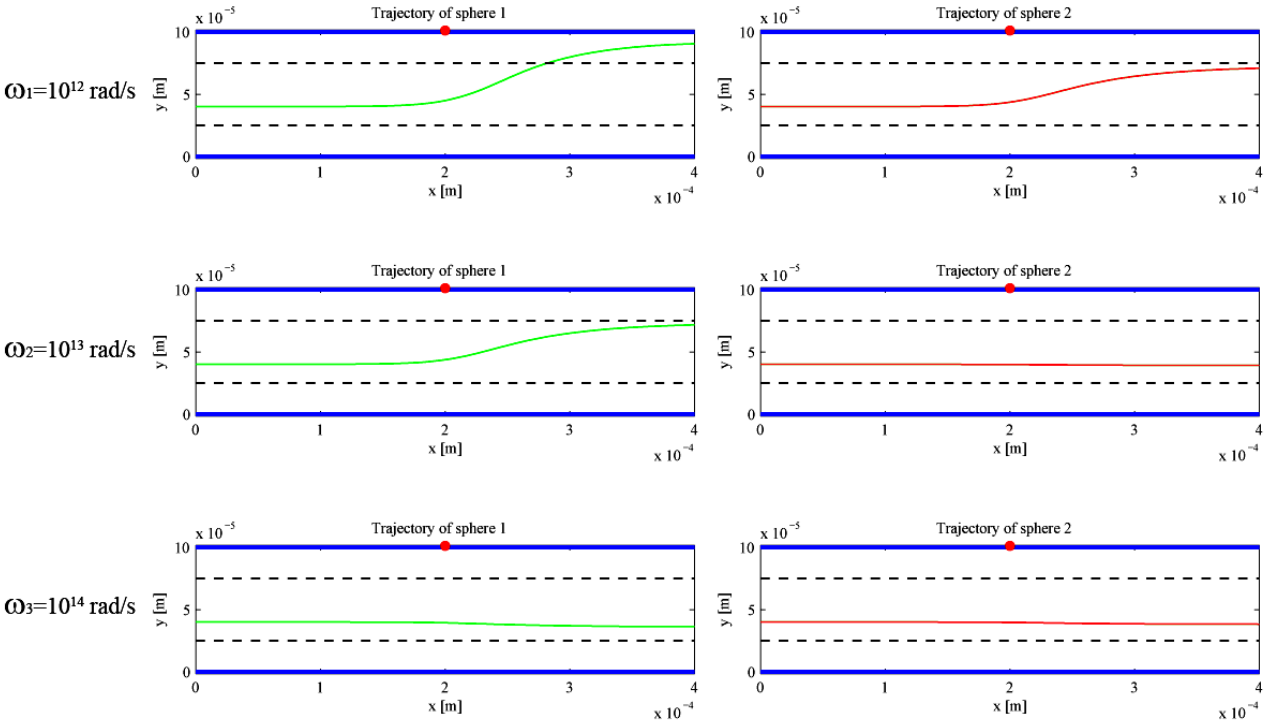

Figure 16: Trajectories of sphere 1 and sphere 2 for three different frequencies $\omega_1 = 10^{12}$ rad/s, $\omega_2 = 10^{13}$ rad/s and $\omega_3 = 10^{14}$ rad/s. The red dot indicates the point electrode, the blue lines are the plates of the microchannel, the dotted lines indicates where the Stokes drag is assumed valid, the green lines are the trajectories of sphere 1 and the red lines are the trajectories of sphere 2.

10 The case of an asymmetric potential

Even though Eq. (80) reveals some interesting results about electrostatic forces on dielectrics in general, it is in itself not of general nature. The assumption of an azimuthal symmetric potential makes it a rather special case, since such a potential is practically non existing in nature. Thus in the general case one has to take into account, that the potential depends on the azimuthal angle, ϕ.

According to [3] the general solution to Laplace's equation in spherical coordinates can then be written as

$$\Phi(r,\theta,\phi) = \sum_{l=0}^{\infty}\sum_{m=-l}^{+l}\left(A_{lm}r^l + \frac{B_{lm}}{r^{l+1}}\right)P_l^m(\cos\theta)e^{im\phi}, \tag{153}$$

where $P_l^m(x)$ is an associated Legendre function defined by

$$P_l^m(x) = (-1)^m(1-x^2)^{m/2}\frac{d^m}{dx^m}P_l(x). \tag{154}$$

Note that from this definition it follows that if $A_m = B_m = 0$ for all $m \neq 0$ Eq. (153) simplifies to the symmetric case Eq. (18). Defining the spherical harmonic functions,

$$Y_{lm}(\theta,\phi) \equiv \frac{1}{N_{lm}}P_l^m(\cos\theta)e^{im\phi}, \tag{155}$$

where

$$\frac{1}{N_{lm}} = \sqrt{\frac{2l+1}{4\pi}\frac{(l-m)!}{(l+m)!}}, \tag{156}$$

is a normalization constant, Eq. (153) can be written as

$$\Phi(r,\theta,\phi) = \sum_{l=0}^{\infty}\sum_{m=-l}^{+l}\left(A_{lm}r^l + \frac{B_{lm}}{r^{l+1}}\right)N_{lm}Y_{lm}(\theta,\phi). \tag{157}$$

The spherical harmonic functions obey the orthonormation integral

$$\int_0^{\pi}\int_0^{2\pi} Y_{lm}(\theta,\phi)Y^*_{l'm'}(\theta,\phi)\sin\theta \mathrm{d}\phi\mathrm{d}\theta = \delta_{ll'}\delta_{mm'}. \tag{158}$$

Here * denotes the complex conjugate.

Like in the symmetric case we assume an applied external potential of the form

$$\Phi_{\mathrm{ext}}(r,\theta,\phi) = \sum_{l=0}^{\infty}\sum_{m=-l}^{+l} A_{lm}r^l N_{lm}Y_{lm}(\theta,\phi). \tag{159}$$

Using exactly the same method as in section 4.2 and exploiting the orthogonality of the spherical harmonics one finds, that the field inside and outside the dielectric sphere is respectively

$$\Phi_{\mathrm{in}}(r,\theta,\phi) = \sum_{l=0}^{\infty}\sum_{m=-l}^{+l}\frac{(2l+1)\epsilon_2}{\epsilon_2(l+1)+\epsilon_1 l}A_{lm}r^l N_{lm}Y_{lm}(\theta,\phi), \tag{160}$$

$$\begin{aligned}\Phi_{\mathrm{out}}(r,\theta,\phi) &= \sum_{l=0}^{\infty}\sum_{m=-l}^{+l} A_{lm}r^l N_{lm}Y_{lm}(\theta,\phi) \\ &\quad -\sum_{l=0}^{\infty}\sum_{m=-l}^{+l} K_l A_{lm}\frac{a^{2l+1}}{r^{l+1}}N_{lm}Y_{lm}(\theta,\phi),\end{aligned} \tag{161}$$

where K_l denotes the usual higher-order Clausius-Mossotti factor. It is seen that in the asymmetric case the induced multipole of order l still turn up in the equation, but now consists of a superposition of $2l+1$ moments of the same order. The strength of these individual moments depend on the the coefficients A_{lm} and N_{lm}.

We see from Eqs. (37) and (160) and Eqs. (38) and (161) , that the potential outside and inside the sphere are of the same form in the azimuthal symmetric and the asymmetric case. Thus we can get the bound charge density by simply replacing the Legendre polynomials, $P_l(\cos\theta)$ in Eq. (49) by $N_{lm}Y_{lm}(\theta,\phi)$

$$\sigma(\theta,\phi) = -\epsilon_0 \sum_{l=0}^{\infty} \sum_{m=-l}^{+l} (2l+1) K_l A_{lm} a^{l-1} N_{lm} Y_{lm}(\theta,\phi). \tag{162}$$

The force on the dielectric sphere when it is present in a dielectric fluid and subject to an externally applied field, $\mathbf{E}_{\text{ext}}(r,\theta,\phi)$, is then in general determined by Eq. (50). Again it is only the externally applied field that can exert a net force on the sphere

$$\mathbf{F}_{\text{DEP}} = \epsilon_r \int_{\partial\Omega} \sigma(\theta,\phi) \mathbf{E}_{\text{ext}}(a,\theta,\phi) \mathrm{d}a \tag{163}$$

Inserting Eqs. (159) and (162) and using $\mathbf{E}_{\text{ext}}(r,\theta,\phi) = -\boldsymbol{\nabla}\Phi_{\text{ext}}(r,\theta,\phi)$ we arrive at

$$\begin{aligned} \mathbf{F}_{\text{DEP}} = {} & \epsilon_0\epsilon_r \sum_{l=0}^{\infty} \sum_{m=-l}^{+l} \sum_{j=0}^{\infty} \sum_{k=-j}^{+j} (2l+1) N_{lm} N_{jk} A_{lm} A_{jk} K_l a^{l-1} \\ & \times \int_{\partial\Omega} Y_{lm}(\theta,\phi) \boldsymbol{\nabla} \left(r^j Y_{jk}(\theta,\phi) \right) \Big|_{r=a} \mathrm{d}a \end{aligned} \tag{164}$$

To obtain an analytical expression of the DEP force in an asymmetric potential one would have to evaluate the integral in Eq. (164) for all three cartesian coordinates. This task is beyond the scope of this report and we cannot guarantee that it is possible to solve the integrals in general at all. Though it seems possible since a check with a computer program like Mathematica reveals that there are constrains on the terms in the quadruple sum of Eq. (164) like in the symmetric case. For the x component of the force, for example, it turns out that the only terms, which are nonzero are the ones for $m+k = \pm 1$ and $l-j=1$. In fact we have been able to verify this analytically for a part of the x component. Since this part involved the integral over three associated Legendre functions, we have evaluated them with the help of the papers [8] and [9].

If one could evaluate the integrals in Eq. (164) in general, one would obtain an expression for the exact DEP force on a dielectric sphere in a asymmetric potential. The potential and the force would then be expressed in terms of the constants A_{lm}, which, if no free charge is present in the region of interest, can be determined for any external potential. The coefficients are found by exploiting the orthogonality of the spherical harmonic functions. Multiplying Eq. (159) with $Y^*_{l'm'}(\theta,\phi)/N_{l'm'}$ and integrating over the surface of the unit sphere gives

$$\int_{\text{unit sphere}} N^{-1}_{l'm'} Y^*_{l'm'}(\theta,\phi) \Phi_{\text{ext}}(r,\theta,\phi) \mathrm{d}a = \int_0^{\pi}\int_0^{2\pi} N^{-1}_{l'm'} Y^*_{l'm'}(\theta,\phi) \Phi_{\text{ext}}(1,\theta,\phi) \sin\theta \mathrm{d}\theta\mathrm{d}\phi. \tag{165}$$

The integral on the right hand side is evaluated by using Eqs. (158) and (159)

$$\sum_{l=0}^{\infty} \sum_{m=-l}^{+l} A_{lm} \frac{N_{lm}}{N_{l'm'}} \int_0^{\pi}\int_0^{2\pi} Y^*_{l'm'}(\theta,\phi) Y_{lm}(\theta,\phi) \sin\theta \mathrm{d}\theta\mathrm{d}\phi = A_{l'm'}. \tag{166}$$

Thus in general the constants, A_{lm}, are given by

$$A_{lm} = \int_{\text{unit sphere}} N_{lm}^{-1} Y_{lm}^{*}(\theta, \phi) \Phi_{\text{ext}}(r, \theta, \phi) \mathrm{d}a. \tag{167}$$

For every known potential $\Phi_{\text{ext}}(r, \theta, \phi)$ of the form Eq. (159) the constants A_{lm} can be found using Eq. (167). This approach is especially useful in cases where the external potential due to a certain electrode configuration can be determined numerically using software like FemLab. The potential will then be known in discrete points in space and the constants A_{lm} can be computed by evaluating the integral in Eq. (167) numerically.

With the constants A_{lm} determined the DEP force on the sphere could be calculated by the exact expression of the DEP force in an asymmetric potential. This would make it possible to evaluate the validity of the lowest-order approximation of the DEP force in any externally applied potential.

11 Conclusion

In this report we have shown that it is possible to derive an exact expression for the DEP force acting upon a dielectric sphere under azimuthal symmetry. The expression found is an infinite sum and can therefore be used with any desired accuracy. Each term in the sum can be interpreted as the force acting on a multipole moment. This is in general the difference between our model and the lowest-order approximation, which only take the force on the dipole moment into account.

We have tested the validity of the lowest-order approximation, and found that it is useful in many cases as long as the applied field is not too inhomogeneous. In cases of very inhomogeneous fields the contribution from the higher-order multipoles is significant, in extreme cases even dominating. In such situations the lowest-order approximation will clearly break down and yield insufficient results.

An approach for handling spherical objects of many layers with different permittivities has also been developed. This approach starts from the solution of the problem of a two layer sphere, which can then be used to solve the problem of many layers by simplifying it in steps. The solution of the two layer sphere is based on introducing an effective permittivity for a two layer sphere, which then can replaced by a one layer sphere. Furthermore we have also found the interval of critical frequencies when working with an AC-potential. To control the sign of the DEP force one should be careful not to choose a driving frequency in this interval.

Even though demonstrated in an very artificial problem, the possibility of continuous separation of spherical objects has been shown. The separation is furthermore frequency dependent and driven by positive or negative DEP forces.

A Cosine law

We want to evaluate $\cos(\sin^{-1}(x))$, so we set $A = \sin^{-1}(x)$. Knowing that

$$\cos^2(A) + \sin^2(A) = 1, \tag{168}$$

we get

$$\cos^2(\sin^{-1}(x)) + x^2 = 1, \tag{169}$$

and thereby

$$\cos(\sin^{-1}(x)) = \pm\sqrt{1 - x^2}. \tag{170}$$

The sign in front of the squareroot clearly depends on the angle A, and one therefore has to analyze the problem at hand when choosing the sign.

B Time-averaging

We define two functions as follows

$$A(t) = \mathrm{Re}\left[A_0 \exp(-i\omega t)\right], \tag{171}$$
$$B(t) = \mathrm{Re}\left[B_0 \exp(-i\omega t)\right]. \tag{172}$$

where A_0 and B_0 are complex amplitudes. We want to calculate the time-average of $A(t)B(t)$ over one full period τ, namely

$$\langle A(t)B(t)\rangle = \frac{1}{\tau}\int_0^\tau A(t)B(t)dt. \tag{173}$$

Using the relation

$$\mathrm{Re}[Z] = \frac{1}{2}\left(Z + Z^*\right), \quad Z \in C, \tag{174}$$

we obtain the following result

$$A(t)B(t) = \frac{1}{4}\left(A_0 \exp(-i\omega t) + A_0^* \exp(i\omega t)\right)\left(B_0 \exp(-i\omega t) + B_0^* \exp(i\omega t)\right) \tag{175}$$
$$= \frac{1}{4}\left(A_0 B_0^* + A_0^* B_0 + A_0 B_0 \exp(-i2\omega t) + A_0^* B_0^* \exp(i2\omega t)\right). \tag{176}$$

Since the period is given by $\tau = 2\pi/\omega$ we have

$$\langle A(t)B(t)\rangle = \frac{1}{4\tau}\left[A_0 B_0^* t + A_0^* B_0 t - \frac{1}{i2\omega}A_0 B_0 \exp(-i2\omega t) + \frac{1}{i2\omega}A_0^* B_0^* \exp(i2\omega t)\right]_0^\tau \tag{177}$$
$$= \frac{1}{4}\left(A_0 B_0^* + A_0^* B_0 + \frac{1}{i4\pi}\left(A_0^* B_0^* - A_0 B_0\right) - \frac{1}{i4\pi}\left(A_0^* B_0^* - A_0 B_0\right)\right) \tag{178}$$
$$= \frac{1}{2}\frac{1}{2}\left(A_0 B_0^* + A_0^* B_0\right) = \frac{1}{2}\mathrm{Re}\left[A_0 B_0^*\right]. \tag{179}$$

The final result is therefore

$$\langle A(t)B(t)\rangle = \frac{1}{\tau}\int_0^\tau A(t)B(t)dt = \frac{1}{2}\mathrm{Re}\left[A_0 B_0^*\right]. \tag{180}$$

C Stokes drag

In the following we will estimate the region in a microchannel were the stokes drag, on a sphere with radius a, is approximately correct. According to [1] the stokes drag on a sphere immersed in steady-state flowing fluid is

$$\mathbf{F}_{\text{drag}} = 6\pi\eta a(\mathbf{v} - \mathbf{u}), \tag{181}$$

where η is the viscosity of the fluid, $\mathbf{v}$ is the velocity of the fluid, a is the radius of the sphere and $\mathbf{u}$ is the velocity of the sphere. Eq. (181) is only valid in a steady-state flow, i.e. the velocity field of the fluid must be constant over the diameter of the sphere. However we consider an ideal Poiseuille flow in an infinite parallel plate channel of height $h = 100$ μm and length L. The velocity field of the fluid in this channel is given by

$$\mathbf{v}(y) = v_x(y)\hat{\mathbf{x}} = \frac{\Delta p}{2\eta L}(h - y)y\hat{\mathbf{x}}, \tag{182}$$

where Δp denotes the pressure difference over the length L. The velocity field of the fluid is a parabola and Eq. (181) will therefore not be valid close to the parallel plates. To find the region where the velocity field is approximately constant over the sphere we can demand

$$\frac{v(y)}{v(y-a)} \in [1-\delta; 1+\delta] \quad \text{and} \quad \frac{v(y)}{v(y+a)} \in [1-\delta; 1+\delta], \tag{183}$$

where δ is the tolerance and $y \in [a; h-a]$. It is important to notice, that we require that both of the ratios should be in the interval $[1-\delta; 1+\delta]$ for a given value of y to be accepted.

We assume that for $\delta = 0.1$ we still can consider Stokes drag to be valid. Setting $a = 3$ μm we get the plot, shown in Fig. (17), of the ratios in Eq. (183).

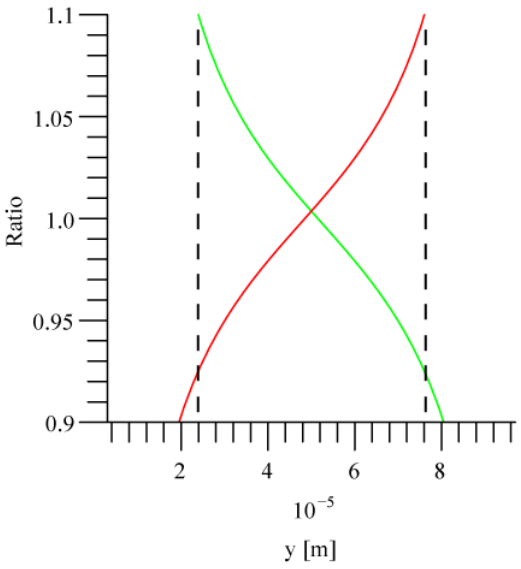

Figure 17: Plot of the ratios

From the figure it can be deduced that both of the ratios in Eq. (183) will be in the desired interval, when $y \in [25; 75]\mu$m. In this region we will therefore assume that Eq. (181) is valid.

D calctraj.m

```
clc
clear all

%Define constants
[vars] = textread('constants.txt','%f','commentstyle','matlab');
l = vars(3);
h = vars(5);
a = vars(9);
pcd = vars(14);
vdt = vars(15);
dt = vars(16);
time = vars(17);

%Options for ode45
options(1) = odeset('Stats','on');
options(2) = odeset('AbsTol',1e-8,'RelTol',1e-8,'Stats','on');
[t u] = ode45(@ode_input,linspace(0,time,vdt),[0 40e-006 0 0],options(2));

for i = 1:length(u)
    if u(i,2) <= a & u(i-1,2) > a
        x = u(i,1);
        k = i;
        lh = 1;
    end
    if u(i,2) >= h-a & u(i-1,2) < h-a
        x = u(i,1);
        k = i;
        lh = 1;
    end
    if u(i,2) > a & u(i,2) < h-a
        lh = 2;
    end
end
lh
switch lh
    case 1
        [tlow ulow] = ode45(@ode_input_low,linspace(0,time,vdt),[u(k,1) a u(k,3) 0],options(2));
        ufinal = [u(1:k-1,:);ulow];
        tfinal = [t(1:k-1,:);tlow];
    case 2
        ufinal = u;
        tfinal = t;
end

%Data for plot of geometri
xbottom = [0,2*l];
ybottom = [0,0];
xtop = [0,2*l];
ytop = [h,h];

%Stokes drag valid
xstokeb = [0,2*l];
ystokeb = [25e-6,25e-6];
xstoket = [0,2*l];
ystoket = [75e-6,75e-6];

%Data for plot of cell
t = linspace(0,2*pi,101);
xcelle = cos(t)*a;
```

```
ycelle = sin(t)*a;

%Plot of trajectory
figure
plot(ufinal(:,1),ufinal(:,2),'g','LineWidth',1)
axis equal
axis([0 2*l -1.5*pcd h+1.5*pcd])
hold on
plot(xbottom,ybottom,'b','LineWidth',3)
plot(xtop,ytop,'b','LineWidth',3)
plot(xstokeb,ystokeb,'k--','LineWidth',1)
plot(xstoket,ystoket,'k--','LineWidth',1)
plot(l,h+pcd,'o','MarkerEdgeColor','r','MarkerFaceColor','r')
xlabel('x [m]')
ylabel('y [m]')
title('Trajectory of sphere 2')
hold off

%Video
figure
for j = 1:length(ufinal)
    plot(xcelle+ufinal(j,1),ycelle+ufinal(j,2),'g','LineWidth',2)
    axis equal
    axis([0 2*l -1.5*pcd h+1.5*pcd])
    hold on
    plot(xbottom,ybottom,'b','LineWidth',3)
    plot(xtop,ytop,'b','LineWidth',3)
    plot(xstokeb,ystokeb,'k--','LineWidth',1)
    plot(xstoket,ystoket,'k--','LineWidth',1)
    plot(l,h+pcd,'o','MarkerEdgeColor','r','MarkerFaceColor','r')
    xlabel('x [m]')
    ylabel('y [m]')
    hold off
    F(j) = getframe;
end
movie(F,0)
movie2avi(F,'film6','compression','Indeo5','fps',24)
```

E ode_input.m

```
function f = ode_input(t,u)

%Define constants
[vars] = textread('constants.txt','%f','commentstyle','matlab');
deltaP = vars(2);
l = vars(3);
nu = vars(4);
h = vars(5);
voltage = vars(6);
q  = vars(7);
eps0 = vars(8);
a = vars(9);
celldensity = vars(10);
i = vars(11);
pcd = vars(14);
L = vars(19);
sigma1 = vars(20);
sigma2 = vars(21);
w = vars(22);

eps1 = vars(12)*eps0;
eps2 = vars(13)*eps0;
m = 4/3*pi*a^3*celldensity;

%Cals s
s = ((l-u(1))^2+(h-u(2)+pcd)^2)^(1/2);

%Calc FDEP for i
F = zeros(1,i);
for n = 1:i
    F(n) = 2*pi*eps2*(q/(4*pi*eps2))^2*1/(s^(2*n+3))*a^(2*n+1)*(n+1)...
        *real(n*(eps1-j*sigma1/w-(eps2-j*sigma2/w))/((eps2-j*sigma2/w)*(n+1)+(eps1-j*sigma1/w)*n));
end
FDEP = sum(F);

%Define output vector
f=[0;0;0;0];

%Fill output vector
f(1:2)=u(3:4);
f(3)=FDEP/m*(l-u(1))/s+6*pi*nu*a/m*(deltaP/(2*nu*L)*(h-u(2))*u(2)-u(3));
f(4)=FDEP/m*(h-u(2))/s-6*pi*nu*a/m*u(4);
```

F ode_input_low.m

```
function f = ode_input_low(t,u)

%Define constants
[vars] = textread('constants.txt','%f','commentstyle','matlab');
deltaP = vars(2);
l = vars(3);
nu = vars(4);
h = vars(5);
voltage = vars(6);
q  = vars(7);
eps0 = vars(8);
a = vars(9);
celldensity = vars(10);
i = vars(11);
pcd = vars(14);
L = vars(19);
sigma1 = vars(20);
sigma2 = vars(21);
w = vars(22);

eps1 = vars(12)*eps0;
eps2 = vars(13)*eps0;
m = 4/3*pi*a^3*celldensity;

%Cals s
s = ((l-u(1))^2+(h-u(2)+pcd)^2)^(1/2);

%Calc FDEP for i
F = zeros(1,i);
for n = 1:i
    F(n) = 2*pi*eps2*(q/(4*pi*eps2))^2*1/(s^(2*n+3))*a^(2*n+1)*(n+1)...
        *real(n*(eps1-j*sigma1/w-(eps2-j*sigma2/w))/((eps2-j*sigma2/w)*(n+1)+(eps1-j*sigma1/w)*n));
end
FDEP = sum(F);

%Define output vector
f=[0;0;0;0];

%Fill output vector
f(1:2)=u(3:4);
f(3)=FDEP/m*(l-u(1))/s+6*pi*nu*a/m*(deltaP/(2*nu*L)*(h-u(2))*u(2)-u(3));
f(4)=0;
```

G constants.txt

```
9.82                    % 1 g
495                     % 2 deltaP
200e-6                  % 3 l
0.604e-3                % 4 nu
100e-6                  % 5 h
0.51                    % 6 voltage
3.8e-13                 % 7 q
8.85e-12                % 8 eps0
3e-6                    % 9 a
1450                    % 10 celldensity
3                       % 11 sum
1.9                     % 12 eps1*eps0 factor - particle
2.2825                  % 13 eps2*eps0 factor - fluid
1e-6                    % 14 point charge depth
240                     % 15 Frames in video
1.5e-3                  % 16 On-off delta time
5e-5                    % 17 total time
1                       % 18 onoff - 1 for on fra start, 2 for off fra start
0.12                    % 19 L
100                     % 20 sigma1 - particle
10e-14                  % 21 sigma2 - fluid
1e14                    % 22 frequency
```

References

[1] H. Bruus. *Theoretical microfluidics*. MIC - Department of Micro and Nanotechnology, second edition, fall 2005. Lecture notes.

[2] W. F. Brown, N. H. Frank, E. C. Kemble, W. H. Michener, C. C. Murdock, and D. L. Webster. The teaching of electricity and magnetism at the college level .1. logical standards and critical issues - report of the coulomb law committee of the aapt. *Am. J. Phys.*, 18(1):1 – 25, 1950.

[3] S. M. Lea. *Mathematics for physicists*. Brooks Cole, first edition, 2003.

[4] E. W. Weisstein. Legendre polynomial. *From MathWorld–A Wolfram Web Resource. http://mathworld.wolfram.com/LegendrePolynomial.html*.

[5] H. Zhou, L. R. White, and R. D. Tilton. Lateral separation of colloids or cells by dielectrophoresis augmented by ac electroosmosis. *J. Colloid. Interf. Sci.*, 285(1):179 – 191, 2005.

[6] D. R. Lide, editor. *Handbook of Chemistry and Physics*. CRC Press, 86th edition, 2005.

[7] B. Dikarev, R. Romanets, V. Bolshakov, and G. Karasev. Influence of emulsion water on conduction in dielectric liquids. *Proceedings of 14" International Conference on Dielectric Liquids (ICDL 2002), Graz (Austria), July 7-12*, 2002.

[8] H. A. Mavromatis and R. S. Alassar. A generalized formula for the integral of three associated legendre polynomials. *Appl. Math. Lett.*, 12(3):101 – 105, 1999.

[9] S. N. Samaddar. Some integrals involving associated legendre functions. *Math. Comput.*, 28(125):257 – 263, 1974.